γ rays from muon capture in ^{27}Al and natural Si

David F. Measday,* Trevor J. Stocki,† Belal A. Moftah,‡ and Heywood Tam§
Department of Physics and Astronomy, University of British Columbia, Vancouver, British Columbia, Canada V6T 1Z1
(Received 13 March 2007; published 27 September 2007)

Muon capture γ rays have been observed for the first time in ^{27}Al, and a significant improvement has been made in the identification of γ-rays from muon capture in natural Si. The $(\mu^-, \nu\gamma)$ reaction was clearly observed in both nuclei and, for ^{28}Si, compares well with calculations. The $(\mu^-, \nu n\gamma)$ reaction was also observed strongly in both nuclei, and the levels which are excited correlate fairly well with the (γ, p) reaction, but not as well with the spectroscopic factors from the $(d,^3\mathrm{He})$ reaction. Some $(\mu^-, \nu 2n\gamma)$, $(\mu^-, \nu 3n\gamma)$, $(\mu^-, \nu p\gamma)$, $(\mu^-, \nu pn\gamma)$, and other reactions have been observed at a lower yield. The Lyman series of the muonic x ray cascades have also been studied.

DOI: 10.1103/PhysRevC.76.035504 PACS number(s): 23.40.−s, 36.10.Dr, 27.30.+t, 21.10.Jx

I. INTRODUCTION

This is the final study of a series of investigations into the γ-ray yields from muon capture in nuclei. Our earlier papers described the results for capture on N [1], Ca, Fe, and Ni [2], and I, Au, and Bi [3]. Muon capture in nuclei is a complex phenomenon which is far from understood, so we have extended our study to two further elements, aluminum, which has not been studied before, and silicon, which has been fairly well studied but we have been able to improve the information quite significantly.

The present situation with regard to muon capture has recently been reviewed by Measday [4]. We shall focus on the experiments which observe the γ rays following the muon capture, which occurs via the weak interactions from the muonic 1s level. Because the mass of the muon is about 106 MeV/c^2, there is plenty of energy available when the muon is absorbed on a proton in the nucleus, and, although the neutrino takes away most of the energy, the product nucleus can be excited to 10 or 20 MeV. In lighter elements the most important reactions are (μ^-, ν) and $(\mu^-, \nu n)$, with $(\mu^-, \nu 2n)$ being only about 5 to 10%, and proton production can reach 10% or more, as is the case for silicon, but for aluminum we shall see that the proton yield is quite low. For heavy nuclides more neutrons are emitted, and almost no protons nor alphas.

For lighter elements such as Al and Si, the nuclear recoil after the neutrino emission causes a significant Doppler broadening for γ rays emitted from levels with a lifetime < 0.5 ps (the slowing down time for the recoilling ion). This Doppler broadening is about 8 keV for a 1 MeV γ ray, already much wider than the detector resolution, and it scales with the energy, so for high energy γ rays, the peak is spread over 30 or 40 keV, which makes it difficult to identify weaker transitions.

Now the capture reactions occur up to a few hundred nanoseconds after the muon stop, so the coincidence requirement is not very stringent in removing background from the experimental area, which is bathed in thermal neutrons; in addition 1 MeV neutrons are produced in the muon capture itself, and so add to the problems. Thus it is critical to measure the γ-ray energies with care and precision. A key advantage that we have is that the energies and branching ratios of γ rays are much better known now (and much more easily accessible from the National Nuclear Data Center). For lighter elements, the γ-ray energies are quite well established, so for the present elements, the energy calibration is better than for our previous spectra. Our γ-ray detector has a somewhat better energy resolution than those used in previous muon capture experiments, but more important is that it is larger and so more efficient for γ rays of a few MeV. Thus an experiment can now identify γ rays of 2 to 6 MeV, even though the yield may be fairly low, and we observe quite a few such γ rays. In addition a modern accelerator like TRIUMF has a macroscopic duty-cycle of 100%, so the data can be taken at a higher rate.

We have studied the muonic x rays because they are useful for energy calibration and for normalization. For ^{27}Al, the energies of the Lyman series have been studied several times and the previous results are in good agreement. The first precise values were those of Schaller *et al.* [5], followed by Fricke *et al.* [6], and finally their definitive compendium [7], which gives the most precise values. For silicon these same authors are in slight disagreement; so we shall assume that the most recent data are the most reliable (the difference is only 0.07 keV, which is not really consequential in our study). For the intensities, we have the observations of Hartmann *et al.* [8] for aluminum, as well as their calculations and those of Vogel [9]. Silicon has been studied by Suzuki [10], and the values are similar to aluminum, which confirms the calculations that indicate very little difference between Mg, Al, P, and S, giving a proportion for the $(2p\text{-}1s)$ transition of about 80% (though the data for P give a slightly lower value, viz. 75%).

For muon capture in aluminum, there are no previously analyzed results, although spectra have been taken by several groups. The neutron multiplicity experiment of MacDonald [11] is very useful to give an overall picture; using the analysis

*Corresponding author: measday@phas.ubc.ca
†Present address: Radiation Protection Bureau, Ottawa, ON, Canada K1A 1C1.
‡Present address: King Faisal Specialist Hospital, Jeddah, Saudi Arabia.
§Present address: California Institute of Technology, Pasadena, CA 91125, USA.

in Measday [4], they find the following yields: zero neutron 9(6)%, one neutron 75(10)%, two neutrons 5(10)% and three neutrons 9(6)%. Note that the reaction ^{27}Al$(\mu^-, \nu pn)^{25}$Na, for example, will be categorized as a one neutron reaction, etc. For the reaction ^{27}Al$(\mu^-, \nu)^{27}$Mg, we could compare to several reactions, but the existing data are not that useful; the reaction ^{27}Al$(n, p)^{27}$Mg has only been studied at 56 MeV [12], which is a little low, and the resolution was only 1.5 MeV, but the data do indicate that the feeding of low-lying levels is very weak, and the first strength comes at an excitation of 6 MeV, which is near where neutron emission becomes possible ($S_n = 6.443$ MeV); the reaction ^{27}Al$(d, {}^2\text{He})^{27}$Mg has been studied [13], but no data have been published. Other reactions such as ^{27}Al$(\pi^-, \gamma)^{27}$Mg and ^{27}Al$(\pi^-, \pi^0)^{27}$Mg have not been studied. For the reaction ^{27}Al$(\mu^-, \nu n)^{26}$Mg we can compare with spectroscopic factors from the reaction ^{27}Al$(d, {}^3\text{He})^{26}$Mg [14], and cross sections for the reaction ^{27}Al$(\gamma, p)^{26}$Mg [15]. For more complex reactions such as $(\mu^-, \nu 2n)$ and $(\mu^-, \nu pn)$, the comparisons are less helpful, but we shall discuss the ^{27}Al$(d, \alpha)^{25}$Mg [16] and ^{27}Al$(\pi^-, 2n)^{25}$Mg [17] reactions.

For silicon, the situation is that there are a multitude of comparisons, so we simplify the discussion. First there exist two previous γ-ray studies of muon capture in silicon. The first was that of Miller *et al.* [18], who gave a complete analysis of γ rays from muon capture in isotopically pure targets of ^{24}Mg and ^{28}Si, using a SiO_2 target. The work of Gorringe *et al.* [19] also used an enriched target of SiO_2 , but focussed exclusively on the reaction ^{28}Si$(\mu^-, \nu\gamma)^{28}$Al, however they identified eight levels, so the comparison is important. For a general picture in ^{28}Si, we again quote the data of MacDonald *et al.* [11]; they find the following yields: zero neutron 36(6)%, one neutron 49(10)%, two neutrons 14(6)%, and three neutrons 1(1)%. This is very different from ^{27}Al, and in spite of the large errors, a difference which is confirmed by our data. Other observations in ^{28}Si are that the reaction ^{28}Si$(\mu^-, \nu)^{28}$Al has a total yield of 26(3)% [18]; this is compatible with the result of MacDonald *et al.* for no neutrons, because we find that the reaction ^{28}Si$(\mu^-, \nu p)^{27}$Mg has a yield of a few percent, and we estimate that the reaction ^{28}Si$(\mu^-, \nu d)^{26}$Mg will similarly have a yield of a few percent; (both would be classified as no neutrons in the experiment of MacDonald *et al.*). Also Sobottka and Wills [20] found that the yield of charged particles was 15(2)%, which is quite large compared to many other nuclei, but comparable to what we observed in ^{40}Ca.

For comparison reactions in ^{28}Si, again we have a surfeit of choices. For the reaction ^{28}Si$(\mu^-, \nu)^{28}$Al, we can compare to the reactions ^{28}Si$(d, {}^2\text{He})^{28}$Al [21,22], and ^{28}Si$(\pi^-, \gamma)^{28}$Al [23], as well as the reaction ^{28}Si$(p, n)^{28}$P [24], which goes to a different nucleus, but because of charge symmetry, exhibits the same yield pattern as the (n, p) reaction. We note that the authors of $(d, {}^2\text{He})$ and (p, n) experiments almost always present their data near 0°, which emphasizes the 1^+ transitions, but an angle of about 12° would have a closer momentum transfer to muon capture. All the data indicate strong feeding of levels at 1373, 1620, 2201, 3105 keV, and around 4.1, 5.2, and 6.1 MeV (using the ^{28}Al energies). This is confirmed by shell-model calculations by Kuz'min and Tetereva [25], who showed that these levels should be excited by both the (p, n) and (μ, ν) reactions. Previous muon capture experiments have detected levels up to 3876 keV, but not above, even though the yield should be quite strong.

For the reaction ^{28}Si$(\mu, \nu n)^{27}$Al, Gorringe *et al.* did not publish an analysis of the ^{27}Al transitions. However we can compare with the spectroscopic factors from the $(d, {}^3\text{He})$ reaction [26], and also with the (γ, p) reaction which exhibits a closer comparison to muon capture [27,28]. For the more complex reactions such as ^{28}Si$(\mu^-, \nu 2n)^{26}$Al, ^{28}Si$(\mu^-, \nu 3n)^{25}$Al, ^{28}Si$(\mu^-, \nu p)^{27}$Mg, ^{28}Si$(\mu^-, \nu pn)^{26}$Mg, ^{28}Si$(\mu^-, \nu p2n)^{25}$Mg, and ^{28}Si$(\mu^-, \nu\alpha)^{24}$Na, the comparison reactions are not as useful, though we shall briefly discuss the reactions ^{28}Si$(d, \alpha)^{26}$Al [29] and ^{28}Si$(\pi^-, 2n)^{26}$Al [17].

II. EXPERIMENT

These data were taken at the same time as our previous data for ^{14}N [1], for Ca, Fe, and Ni [2], and for I, Au, and Bi [3], so we shall simply outline the technique. The setup is illustrated in Fig. 1. The experiment was performed on beamline M9B at TRIUMF. The beamline includes a 6 m, 1.2 T superconducting solenoid in which a 90 MeV/c π^- beam decays into muons. The resulting backward μ^- are then separated from the pions by a bending magnet, and pass through a collimator into the experimental area. The collimator was made of lead, but lined with polyethylene to reduce the number of neutrons and γ rays from muons stopping in the collimator. The beam rate was about 2×10^5 s^{-1}, with negligible pions, but with ~20% electrons. The muon beam is somewhat diffuse, so a muon stopping in the target is selected by three plastic scintillators, two before and one large one in anticoincidence after the target. The defining counter, just before the target was 51 mm in diameter. The counters were wrapped in aluminum foil with black electrical tape, which is made of polyvinyl chloride (PVC). Many muons stop in the defining counter, mainly in the carbon, but some in the aluminum and also in the chlorine.

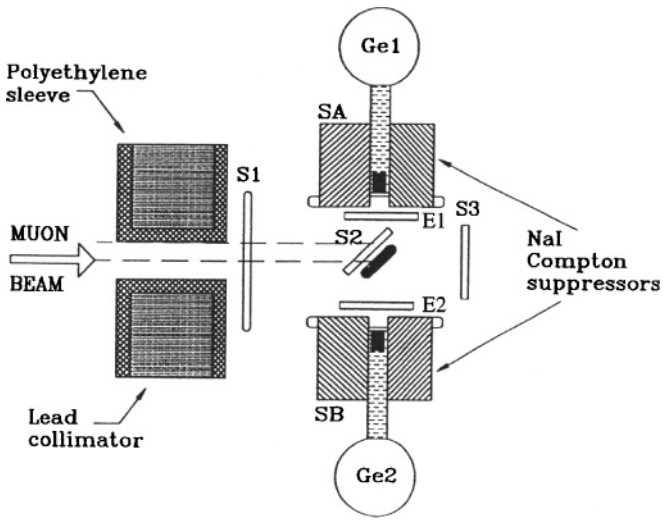

FIG. 1. The experimental setup, showing the alignment of the HPGe detectors at right angles to the muon beam. Only the larger detector was analyzed in detail as it had a count rate three times that of the smaller detector.

The targets consisted of powders of the pure elements. There seems to have been a fair amount of oxide present, as the oxygen muonic ($2p$-$1s$) x ray is quite clear in all spectra.

There were always two HPGe γ-ray detectors at right angles to the beam line, but only the larger detector was used in the analysis. For the Al and Si targets, we used what is called locally the Toronto detector; it is a p-type detector and has an efficiency of 37.5%. It has a timing resolution of about 7 ns, and an in-beam resolution of 3 keV at 1.3 MeV, 5 keV at 2.8 MeV, and 10 keV at 6.1 MeV. It had a NaI(Tl) Compton suppression anticoincidence shield, but this was not used, because it can introduce efficiency concerns for cascading transitions. However for silicon, we had access to the muon capture spectra taken by Moftah for his Ph.D. thesis [30]; this work was mainly focussed on the 1229 keV γ ray from the 2201 keV level [31], but general spectra were obtained as well. These data had the Compton suppression working strongly, and were very useful in the present study in ensuring that escape peaks were correctly identified. In front of both the HPGe detectors, there was a plastic scintillator to tag electrons entering the detector. The electronics consisted of standard spectroscopic amplifiers and timing filter amplifiers, followed by constant fraction discriminators. The event trigger was a HPGe pulse above a hardware discriminator at typically 100 keV. The closest muon was selected from a delayed signal from the plastic defining scintillators. Information recorded for each event included the pulse heights in the two HPGe detectors and the defining plastic scintillator, as well as timing information. Each event was read by a starburst and a VAXstation 3200, and written to tape. Over 100 online histograms were kept for every target in order to monitor the progress of the experiment. The cuts could be reanalyzed offline, but the histograms had been well chosen, and this was rarely done. For the analysis of the γ-ray spectra, we chose the total histogram, so x rays and γ rays were together, thus improving the energy calibration, and efficiency measurements. If there was an overlap, the events in coincidence with the muon stop could be selected to give a purer x-ray spectrum. Even though the muon capture occurs over 1.5μs, the x-ray spectrum normally had some γ-ray content, and vice versa.

III. DATA ANALYSIS

The identification of a γ ray is via its energy only. The stability of the amplifiers was quite remarkable and the gain changed by less than one channel in 1000 over several days. Thus for both these elements, we summed several spectra to give a spectrum with much better statistical significance. We took the energy calibration from each spectrum itself. For the energy calibration the histogram was divided into sections and a quadratic form was taken for the energy-channel relationship and it was fitted to at least four calibration lines. The spectra consisted of 2048 channels, and for our medium gain spectrum at 1.3 keV per channel, the sections would typically be 100–700, 700–1300, 1300–2000, and 2000–2700 keV. For the low gain spectrum at 5.3 keV per channel, the sections were typically 100–1400, 1400–2200, and 2200–10850 keV. Only the highest energy section was used to define yields; below 2.5 MeV, the yields were taken from the medium gain spectrum. The energy calibration was good to about 0.1 keV up to 2.5 MeV, and deteriorated somewhat above this. The calibration was better than previous data because of the better statistics, and the larger number of well established lines that could be used for the energy calibration. The thermal neutron (n, γ) lines were noticeable for these elements, because of the longer timing gate, but only ^{56}Fe(n, γ) was sufficiently clear to use as a calibration line, and as the pair at 7.6 MeV are quite high in energy, these are very useful. Typical calibration lines are given in Table I. They are known better than could be utilized in this experiment. Note that the energy given here is the γ-ray energy, not the transition energy, which can be a little higher because of the recoil correction.

TABLE I. Gamma-ray and muonic x ray energies used for calibration, taken from Measday [4], NNDC [14], Helmer and van der Leun [32], Dewey *et al.* [33], Raman [34], and Revay [35].

Line	Energy(error) in keV	Ref.
μ-mesic O($2p$-$1s$)	133.535(2)	[4]
μ-mesic Al($2p$-$1s$)	346.828(2)	[4]
μ-mesic Si($2p$-$1s$)	400.177(5)	[4]
Annihilation	510.991 2(14)[a]	[4]
^{25}Mg	585.08(2)	[14]
^{27}Al	843.74(3)	[14]
^{28}Al	941.72(4)	[14]
^{25}Mg	974.83(2)	[14]
^{27}Al	1014.42(3)	[14]
^{26}Mg	1129.58(5)	[14]
^{60}Ni (from ^{60}Co β decay)	1173.228(3)	[32]
^{41}Ar	1293.586(7)	[14]
^{60}Ni (from ^{60}Co β decay)	1332.492(4)	[32]
^{24}Mg	1368.633(6)	[14]
^{27}Mg	1698.57(5)	[14]
^{28}Si (from ^{28}Al β decay)	1778.969(12)	[14]
^{26}Mg	1808.66(3)	[14]
$np \rightarrow \gamma d$	2223.248 4(4)	[33]
^{24}Mg (from ^{24}Na β decay)	2754.03(2)	[14]
^{26}Mg	2938.16(4)	[14]
^{16}N	6129.14(3)	[4]
^{56}Fe(n, γ)[b]	7645.55(3)	[34]
	7645.49(9)	[35]

[a]This energy is 7.7(14) eV below the mass of the electron [36].
[b]A partially resolved doublet, with another line at 7631.1 keV.

For muon capture yields, many levels have two or more deexciting transitions. If we have a marginal observation of a single γ ray, we normally do not mention it, but if we have a marginal identification of two, or even better three, transitions, then we consider this better evidence.

The relative efficiency of the detector was obtained with a ^{152}Eu source for which the intensities are well known between 122 and 1408 keV [14,37], see Fig. 2. We also used ^{133}Ba as a check at the lower energies. For the higher energies we obtained the energy dependence of the efficiency by using the bismuth muonic x rays with a check with iodine x rays [3]. Above 900 keV, we used the standard form of

$$\ln(\text{eff}) = 0.200\text{–}0.780 \ln E_\gamma \text{ (MeV)}. \quad (1)$$

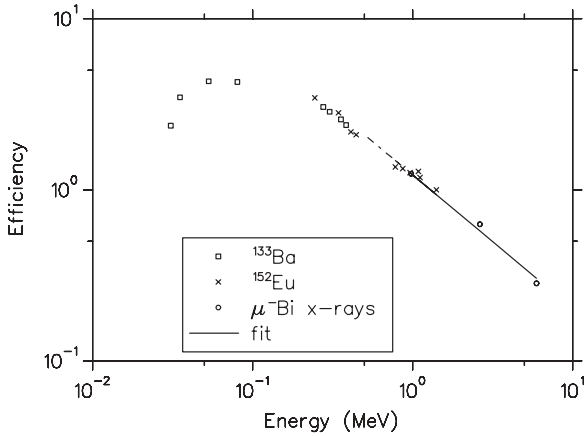

FIG. 2. The efficiency curve for the HPGe detector used in this experiment, using ^{133}Ba and ^{152}Eu sources [14,37], plus iodine and bismuth ($2p$-$1s$) muonic x rays [3].

Note that this value for the Toronto detector is the same as used for our I, Au, and Bi paper [3], but slightly different from the Ca, Fe, and Ni publication because we had reanalyzed the data for the cascade of the bismuth muonic x rays, which define the high energy efficiency. It affects only the γ rays above 2 MeV, and would not make a significant difference to our results for Ca, Fe, or Ni [2].

IV. RESULTS FOR ALUMINUM

To illustrate the complexity of a spectrum, we present in Fig. 3 the range 550 to 900 keV for aluminum. The only major capture line is the large peak at 585 keV which comes from ^{25}Mg and has a yield of 3.3%. In addition there are three neutron edges at 595.8 keV from ^{74}Ge, 691.4 keV from ^{72}Ge, and 834.0 keV also from ^{72}Ge, a background ($2p$-$1s$) muonic line from chlorine at 579 keV, and a major background line at 844 keV, caused by the reaction ^{27}Al(n, n') as well as ^{27}Mg beta decay. Furthermore the line at 787 keV has not been identified. The neutron induced triangles are a major feature in our spectra and need to be understood, so several independent investigations have been made [38,39].

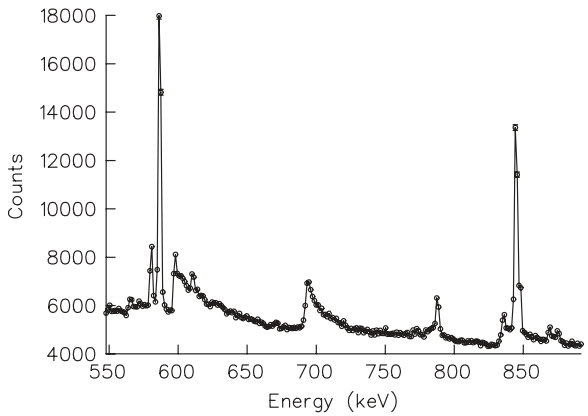

FIG. 3. The spectrum for ^{27}Al at low energy to illustrate neutron effects on the HPGe detector. Neutron edges are at 595.8 keV from ^{74}Ge, 691.4 keV from ^{72}Ge, and 834.0 keV also from ^{72}Ge. The only muon capture line is the large peak at 585 keV from ^{25}Mg, which has a yield of 3.3% and is produced in the reaction ^{27}Al$(\mu^-, \nu 2n\gamma)^{25}$Mg. The line at 787 keV has not been identified.

TABLE II. The muonic Lyman (or K) series for aluminum, giving the observed energy and the absolute intensity per muon stop, normalized to 100% for the sum of this series. We compare to previous results for the energies [5–7] and intensities [8].

μ x ray	Energy (keV) (this exp.)	Energy (keV) [5–7]	Intensity (%) (this exp.)	Intensity (%) [8]
$2p$-$1s$	346.828[a]	346.828(2)	79.8(8)	79.65(60)
$3p$-$1s$	412.87(5)	412.877(10)	7.62(15)	7.43(29)
$4p$-$1s$	435.96(10)	435.981(12)	4.87(10)	4.72(20)
$5p$-$1s$	446.61(10)	446.65(4)	3.86(10)	3.89(17)
$6p$-$1s$	452.38(10)	452.45(5)	2.20(10)	2.35(11)
(7 to ∞) p-$1s$			1.63(15)	1.96(20)

[a]This energy was used as a calibration [5].

We shall first discuss the muonic x rays in aluminum. These results are used in the overall normalization of the muon capture γ rays; however they are also interesting in their own right. Our results for the Lyman series are given in Table II, and are compared to the previous energies of Fricke *et al.* [5], Fricke *et al.* [6], and Schaller *et al.* [7]. The results are all given as the center of gravity, so the results of Fricke *et al.* [6] were adjusted slightly. The ($5p$-$1s$) and ($6p$-$1s$) energies were calculated from point nucleus values, by using the observed finite size correction for the ($4p$-$1s$) x ray of Fricke *et al.* [6]. The intensities are those of Hartmann *et al.* [8]. Their value for the K_β/K_α had been given before [40] and compared to earlier results. For both our results and those of Hartmann *et al.*, it is assumed that the sum of the Lyman series is 100% of the muon stops in aluminum. For all the data, both energies and intensities, the agreement is excellent. We shall use for the yield normalization, our own value of 79.8(8)% for the intensity of the ($2p$-$1s$) x ray.

We now turn to capture γ rays. For the normalization, we shall use the rates given in Table III, taken from Suzuki *et al.* [41]. Note that the number of ($2p$-$1s$) x rays is similar to our previous data for calcium, but 60 to 200 times more than for the other elements.

We shall first discuss the reaction ^{27}Al$(\mu^-, \nu\gamma)^{27}$Mg, and we present our γ-ray yields in Table IV. Note that we have not

TABLE III. Values of the parameters for muon capture in aluminum and silicon taken from Suzuki *et al.* [41].

Quantity	Aluminum	Silicon
Muonic lifetime (ns)	864(2)	758(2)
Muonic capture rate (s^{-1})	$705(3) \times 10^3$	$868(3) \times 10^3$
Decay rate (s^{-1})	452×10^3	451.5×10^3
Capture probability (%)	60.9	65.8
Target material	elemental powder	elemental powder
Counts for the ($2p$-$1s$) x ray	1.3×10^6	2.1×10^6

TABLE IV. Observed γ-ray yields, per muon capture, for the reaction ^{27}Al$(\mu^-, \nu\gamma)^{27}$Mg. The transition energies have been calculated from the newly recommended values for the level energies [14].

Level in ^{27}Mg (keV)	J^π	Transition branching ratio (%)	Transition energy (keV)	Observed γ-ray yield (%)
984.92	$1/2^+$	100	984.90	3.2(2)
1698.63	$5/2^+$	100	1698.57	2.0(2)
1940.35	$5/2^+$	33	1940.28	0.60(7)
		66	955.41	1.26(6)
3476.33	$1/2^+$	98	3476.09	1.0(3)
3760.4(1)	$7/2^-$	100	2061.69	0.15(11)
4552.8(6)	$(3/2, 5/2)^+$	25	3567.6	0.14(14)
		52	2612.3	0.23(14)
4828.14(4)	$(1/2, 3/2)^-$	35	4827.7	0.1(1)
		51	3842.9	<0.2
5627(1)	$(3/2, 5/2)^+$	42	5626.4	1.4(4)
		30	3686.4	1.5(6)
		18	3928.1	0.53(27)

used the transition energies for ^{27}Mg exactly as given by the NNDC [14] in the second half of their tabulation, but we have recalculated the energies from the newly recommended values for the levels. We have also done this for ^{25}Mg; for ^{26}Mg the difference in insignificant.

In Table V, we take account of the transition branching ratios, and subtract known cascading to give the direct excitation of the level in the reaction ^{27}Al$(\mu^-, \nu)^{27}$Mg. Note that the cascading is always a lower limit, as more transitions to each level can come from weaker unobserved γ rays.

The total yield for γ rays from the reaction ^{27}Al$(\mu^-, \nu)^{27}$Mg is 9.7(11)%, which is low for a light element, especially as we do not expect a significant ground state transition either, but consistent with the neutron multiplicities of MacDonald *et al.* [11]. The high yield of the 5627 keV level is consistent with the (n, p) reaction [12], which detected a strong peak at about 6 MeV. As they detected a very low yield for lower energy levels, we suspect that our γ ray yields for the levels at 985, 1699, 1940, and even 3760 keV are mainly from cascades coming from unobserved transitions from levels from 5700 keV up to neutron threshold at 6443 keV.

TABLE V. Deduced values for the direct excitation of levels from the reaction ^{27}Al$(\mu^-, \nu)^{27}$Mg, taking account of the transition branching ratios and known cascading from Table IV.

Level in ^{27}Mg (keV)	Known cascading (%)	Direct yield per muon capture (%)
984.92	0.36(7)	2.8(2)
1698.63	0.9(2)	1.1(3)
1940.35	1.33(3)	0.53(31)
3476.33	0.20(5)	0.8(3)
3760.4(1)	–	0.15(11)
4552.8(6)	–	0.44(27)
4828.14	0.04(1)	0.16(20)
5627(1)	–	3.8(9)

TABLE VI. Observed γ-ray yields, per capture, for the reaction ^{27}Al$(\mu^-, \nu n\gamma)^{26}$Mg.

Level in ^{26}Mg (keV)	J^π	Transition branching ratio (%)	Transition energy (keV)	Observed γ-ray yield (%)
1808.73	2^+	100	1808.66	51(5)
2938.34	2^+	9	2938.16	1.1(2)
		91	1129.58	14.8(15)
3588.56	0^+	100	1779.77	0.65(20)
3941.55	3^+	38	2132.73	1.3(2)
		62	1003.19	2.3(2)
4318.88	4^+	100	2510.02	8.7(7)
4332.57	2^+	79	2523.71	2.8(8)
		15	1394.19	0.5(2)
4350.08	3^+	52	2541.22	1.7(5)
		48	1411.70	2.3(4)
4835.13	2^+	85	1896.72	2.6(2)
4901.30	4^+	94	3092.37	1.3(3)
4972.29	0^+	93	2033.87	0.4(1)
5291.74	2^+	88	2353.29	1.2(2)
5476.11	4^+	14	3667.10	0.2(2)
		29	1534.51	0.3(3)
		57	1157.20	0.40(14)
5691.11	1^+	61	3882.07	0.50(25)
		28	2752.61	0.5(5)
7824(3)	3^-	40	4885(3)	0.45(15)
		40	3882(3)	0.50(25)
8052.9(6)	2^-	100	6243.4(6)	<0.45
8705.73(9)	4^+	29	4763.71(10)	<0.22
		45	4386.45(11)	<0.6
9044.7(3)	2^-	100[a]	6106.4[a]	<0.3

[a]Taken from an earlier compilation, not the present NNDC compilation [14], thus doubtful.

We shall now discuss the reaction ^{27}Al$(\mu^-, \nu n\gamma)^{26}$Mg, and we present our γ-ray yields in Table VI. The number of observed levels is quite large. Between the 5691 and 7824 keV levels, there are a few tentative identifications, at or below a yield of 0.5%, but we do not list them here.

We illustrate a major complication in Fig. 4, showing the overlap of three lines from the reaction ^{27}Al$(\mu^-, \nu n\gamma)^{26}$Mg. The smaller peak at 2353 keV is also from ^{26}Mg and indicates the normal triangular shape for neutron production reactions. The region 2490 to 2550 contains three major transitions from the levels at 4319, 4333, and 4350 keV; the largest yield (8.7%) is at 2510 keV, next is the medium one (2.8% yield) hidden at 2524 keV, and the smallest (1.7% yield) at 2541 keV. As the peaks are nonstandard in shape, we assume the peaks are all symmetrical, and use the simple method of obtaining the yield of the 2510 line by integrating from 2485 keV up to the top of the peak, and doubling it, then similarly integrating down from 2555 keV to the peak at 2541 keV, and doubling it, then finally subtracting these two yields from the total integrated yield from 2485 until 2555 keV,

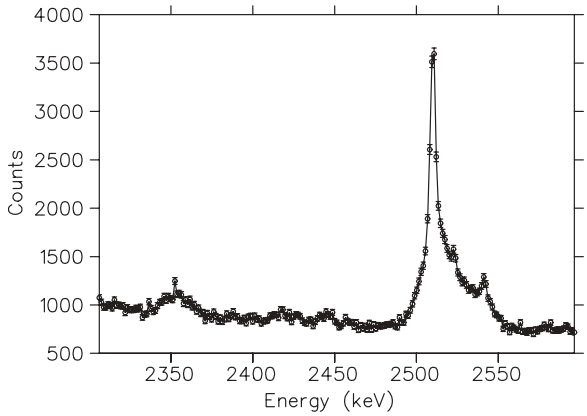

FIG. 4. The spectrum for ^{27}Al at the overlapping triplet. Neutron emission reactions give a triangular Doppler shift as seen at 2353 keV, but the γ-ray transitions from the reaction ^{27}Al(μ^-, $\nu n\gamma$)^{26}Mg at 2510, 2524, and 2541 keV overlap because of the Doppler shift. However the separate yields can be obtained with some confidence.

thus obtaining the yield of the middle triangle at 2524 keV. We believe this method is more dependable than any fitting would be. Of course we are vulnerable to any hidden unknown line, but that is always a problem for any situation.

In Table VII, we take account of the transition branching ratios, and subtract known cascading to give the direct excitation of the levels in the reaction ^{27}Al(μ^-, $\nu n\gamma$)^{26}Mg. We compare with spectroscopic factors from the reaction ^{27}Al(d,^{3}He)^{26}Mg [14,42], and integrated cross sections from the reaction ^{27}Al(γ, p)^{26}Mg from Thomson [43], and from Ryan *et al.* [15]. The data of Thomson were from a γ-detection experiment, integrating the incident photon energy from 16 to 24 MeV, and are quoted by Ryan *et al.* Their own data used proton detection, and this is an integration from 14.8 to 27.6 MeV incident photon energy. We see that our own data correlate well with the (γ, p) reaction, and not so well with the spectroscopic factors, although if the spectroscopic factor is large, we see a strong yield for that level. If we take the first nine excited states, we obtain a correlation coefficient of $r = 0.85$ for the spectroscopic factors, and $r = 0.90$ for the (γ, p) results of Thomson [43].

From these data we estimate that the ground state yield in muon capture is about 4%, and so we obtain a total observed yield of 57% for the reaction ^{27}Al(μ^-, νn)^{26}Mg, also in fair agreement with the neutron multiplicities of MacDonald *et al.* [11], again remembering that they include other reactions, and we are certainly missing some γ rays. We note that a useful visual impression of the spectroscopic factors is presented in Fig. 1 from Sada *et al.* [44], who studied the reaction ^{27}Al(γ, p)^{26}Mg at $E_\gamma = 50$ MeV with an energy resolution of 500 keV. A similar spectrum is given by Ireland *et al.* [45] for $E_\gamma = 60$ MeV. For such high energy γ rays, the yields of this reaction approximate the spectroscopic factors, unlike the yields over the giant dipole resonance. Thus we note that in addition to the strong feeding of the levels at 1809 and

TABLE VII. Deduced values for the direct excitation of levels from the reaction ^{27}Al(μ^-, νn)^{26}Mg, taking account of the transition branching ratios and known cascading from Table VI. We compare with results of the spectroscopic factors from the reaction ^{27}Al(d,^{3}He)^{26}Mg [14,42] (correlation coefficient $r = 0.85$), and integrated cross sections from the reaction ^{27}Al(γ, p)^{26}Mg [15,43] ($r = 0.90$).

Level in ^{26}Mg (keV)	Known cascading (%)	Direct yield per muon capture (%)	Spectroscopic factors [42]	^{27}Al(γ, p)^{26}Mg [43]	^{27}Al(γ, p)^{26}Mg [15]
0	53(5)	{4}[a]	0.45	–	0.60(6)
1808.73	32(2)	19(6)	1.5	2.00(50)	1.61(17)
2938.34	9.8(6)	5.7(2)	0.33	0.74(15)	0.9(2)
3588.56	–	0.65(20)	0.009	0.32(10)[b]	fixed at 0
3941.55	0.77(26)	2.8(3)	0.03	–	fixed at 0
4318.88	0.46(15)	8.2(7)	–	1.5(2)	2.7(6)[c]
4332.57	0.04(2)	3.50(10)	–	<0.25	included[c]
4350.08	–	4.4(7)	0.18	0.5(2)	included[c]
4835.13	–	3.06(20)	0.14, 0.12	0.63(15)	1.4(5)[d]
4901.30	–	1.38(30)	0.024	<0.2	included[d]
4972.29	–	0.43(10)	0.003	–	included[d]
5291.74	–	1.36(28)	0.01	–	–
5476.11	–	0.8(3)	0.032	–	–
5691.11	–	1.0(6)	0.045	–	–
7824(3)	–	1.2(6)	1.2	–	–
8052.9(6)	–	<0.45	0.11	–	–
8705.73(9)	–	<1.0	0.18	–	–
9044.7(3)	–	<0.3	0.75	–	–

[a]Estimate using the data from the (γ, p) reaction.
[b]This assignment is uncertain [15].
[c]Because of the energy resolution, the datum includes three levels viz. 4319, 4333, and 4350 keV.
[d]Because of the energy resolution, the datum includes three levels viz. 4835, 4901, and 4972 keV.

TABLE VIII. Observed γ-ray yields, per capture, for the reaction $^{27}\mathrm{Al}(\mu^-, \nu 2n\gamma)^{25}\mathrm{Mg}$. The transition energies have been calculated from the newly recommended values for the level energies [14].

Level in ^{25}Mg (keV)	J^π	Transition branching ratio (%)	Transition energy (keV)	Observed γ-ray yield (%)
585.09	$1/2^+$	100	585.08	3.34(34)
974.85	$3/2^+$	51	974.83	1.39(14)
		49	389.76	1.34(13)
1611.77	$7/2^+$	100	1611.71	2.2(6)
1964.61	$5/2^+$	26	1964.53	0.41(7)
		47	1379.48	0.59(6)
		27	989.74	0.32(17)
2563.44	$1/2^+$	80	1978.27	$<$0.2
2737.7	$7/2^+$	87	1762.8	0.24(10)

4350 keV, there is feeding of levels at 7860, 9080, and 11200 keV. As ^{26}Mg is bound up to 11093 keV, the first two should be detected in muon capture, and maybe some of the structure at 11200 keV because of the energy resolution in that experiment. The difficulty is that the γ-ray branching ratios are not available for the 9080 keV peak, although an earlier compilation gave a level at 9044.7 keV as cascading 100% to the 2938 keV level.

We shall now discuss the reaction $^{27}\mathrm{Al}(\mu^-, \nu 2n\gamma)^{25}\mathrm{Mg}$, and we present our γ-ray yields in Table VIII. The number of observed levels is much less than for the $^{27}\mathrm{Al}(\mu^-, \nu n\gamma)^{26}\mathrm{Mg}$ reaction, but still significant. Above the level at 2737.7 keV, we are able to limit the yield of about another ten transitions, each one being less than 0.4%.

In Table IX, we take account of the transition branching ratios, and subtract known cascading to give the direct excitation of the level in the reaction $^{27}\mathrm{Al}(\mu^-, \nu 2n)^{25}\mathrm{Mg}$. Our total of observed yield for the reaction $^{27}\mathrm{Al}(\mu^-, \nu 2n\gamma)^{25}\mathrm{Mg}$ is 7.3(7)%, and we compare with the reaction $^{27}\mathrm{Al}(d, \alpha)^{25}\mathrm{Mg}$, using Table III of Sheline and Harlan [16], who used about 8 MeV deuterons and list the yields at 130°. This is, of course, a rough comparison, but both reactions excite most of the lower levels fairly uniformly. We use this comparison to estimate

TABLE IX. Deduced values for the direct excitation of levels from the reaction $^{27}\mathrm{Al}(\mu^-, \nu 2n)^{25}\mathrm{Mg}$, taking account of the transition branching ratios and known cascading from Table VIII. We compare with results of the reaction $^{27}\mathrm{Al}(d, \alpha)^{25}\mathrm{Mg}$ [16] for α particles at 130° from 8 MeV deuterons.

Level in ^{25}Mg (keV)	Known cascading (%)	Direct yield per muon capture (%)	Yield from $^{27}\mathrm{Al}(d, \alpha)^{25}\mathrm{Mg}$
0	7.3(7)	3(1)[a]	0.73
585.09	1.97(12)	1.37(35)	0.25
974.85	0.64(11)	2.09(22)	0.50
1611.77	–	2.2(6)	0.79
1964.61	–	1.33(11)	0.75
2563.44	–	$<$0.25	0.26
2737.7	–	0.28(11)	0.49

[a]Estimate using the (d, α) reaction.

TABLE X. Observed γ-ray yields, per capture, for the reaction $^{27}\mathrm{Al}(\mu^-, \nu 3n\gamma)^{24}\mathrm{Mg}$.

Level in ^{24}Mg (keV)	J^π	Transition branching ratio (%)	Transition energy	Observed γ-ray yield (%)
1368.68	2^+	100	1368.63	1.3(2)[a]
4122.87	4^+	100	2754.01	0.2(2)[a]
4238.36	2^+	78	4237.96	$<$0.4
		22	2869.50	$<$0.1
5235.20	3^+	97	3866.19	$<$0.25

[a]We have subtracted off a contribution of 0.2% from a background of ^{24}Na decay.

the ground-state transition in muon capture to be 3(1)%. The $(\pi^-, 2n)$ reaction detects only the 585 keV line [17].

Even the reaction $^{27}\mathrm{Al}(\mu^-, \nu 3n\gamma)^{24}\mathrm{Mg}$ is detected, albeit at low yield, and we present our γ-ray yields in Table X.

We observe 1.5% yield for the reaction $^{27}\mathrm{Al}(\mu^-, \nu 3n\gamma)^{24}\mathrm{Mg}$, and if the ground state transition were 3%, and an additional 1.5% is unobserved, we obtain an estimated total for this reaction of 6%, compatible with MacDonald *et al.* [11].

We see very little evidence for more complex reactions. For the reaction $^{27}\mathrm{Al}(\mu^-, \nu p\gamma)^{26}\mathrm{Na}$, we set limits of 0.1% on the first two levels above 100 keV. For the reaction $^{27}\mathrm{Al}(\mu^-, \nu pn\gamma)^{25}\mathrm{Na}$, we set limits of 0.2% on the first three levels above 100 keV. For the reaction $^{27}\mathrm{Al}(\mu^-, \nu p2n\gamma)^{24}\mathrm{Na}$, we clearly detect the first level at 472 keV with a yield of 0.50(5)%. However the reaction $^{23}\mathrm{Na}(n, \gamma)^{24}\mathrm{Na}$ is detected in other spectra, including the 472 keV γ ray; we also had a small magnesium contamination which might contribute too; thus we estimate that at least half, if not more, of the yield in the aluminum spectrum is background. Similarly for the reaction $^{27}\mathrm{Al}(\mu^-, \nu p3n)^{23}\mathrm{Na}$, we detect the first level at 440 keV with a yield of 0.6(2)% and maybe the level at 2391 with a yield of 0.25(20)%, but these can also occur from the reaction $^{23}\mathrm{Na}(n, n')^{23}\mathrm{Na}$, and the 440 keV γ ray is detected in other spectra, albeit at a slightly lower equivalent yield of 0.2%, so again we estimate that at least half of these yields in the aluminum spectrum are background. Similarly for the α-producing reactions, for $^{27}\mathrm{Al}(\mu^-, \nu\alpha\gamma)^{23}\mathrm{Ne}$ we set limits for the yields of $<$0.3% on the first three levels, and for $^{27}\mathrm{Al}(\mu^-, \nu\alpha 2n\gamma)^{21}\mathrm{Ne}$ potential γ rays are hidden by more prolific lines; but for the reaction $^{27}\mathrm{Al}(\mu^-, \nu\alpha n\gamma)^{22}\mathrm{Ne}$, we clearly detect the γ ray at 1274.5 keV with an apparent yield of 2.0(2)%, but this can also occur from ^{22}Na decay which is clearly detected in our background runs, and in other spectra, but again normally at a lower yield of 0.5% or less; thus all we can state is that the yield of this γ ray in muon capture is $<$2%. In summary, all proton and alpha producing reactions have a very low yield of γ rays, and probably each one below 1 or 2%, which is much less than for ^{28}Si or ^{40}Ca.

We can now estimate the overall picture for muon capture in ^{27}Al, using all the information available. One useful extra constraint is the activation experiment of Wyttenbach *et al.* [46] which obtained a yield of 2.8(4)% for the reaction $^{27}\mathrm{Al}(\mu^-, \nu pn)^{25}\mathrm{Na}$, and 0.76(11)% for the reaction $^{27}\mathrm{Al}(\mu^-, \nu\alpha)^{23}\mathrm{Ne}$. We emphasize that many of the values in

TABLE XI. Summary of the yield (in %) of all possible muon capture reactions in ^{27}Al.

Reaction	Observed γ-ray yield	Estimated ground-state transition	Missing yields	Total yield
^{27}Al$(\mu^-, \nu)^{27}$Mg	10(1)	0	3	13
^{27}Al$(\mu^-, \nu n)^{26}$Mg	53(5)	4	4	61
^{27}Al$(\mu^-, \nu 2n)^{25}$Mg	7(1)	3	2	12
^{27}Al$(\mu^-, \nu 3n)^{24}$Mg	2	3	1	6
^{27}Al$(\mu^-, \nu pxn)^{26\text{-}23}$Na	2	2	1	5
^{27}Al$(\mu^-, \nu \alpha xn)^{23\text{-}21}$Ne	1	2	0	3
Total	75(5)	14	11	100

Table XI are rough estimates, but the exercise is useful because the sum must be 100%.

V. RESULTS FOR SILICON

As indicated in the introduction, silicon has been studied before, so we can compare our results with many previous experiments. First we present our data for the Lyman series of the muonic x rays. In Table XII, we give our observed energies and intensities for natural silicon, compared to previous experiments.

For the energies, the comparison with previous experiments is complex. First, for the $(2p\text{-}1s)$ transition, the best result is that of Fricke *et al.* in their compendium [7]; but they give the result for the isotope ^{28}Si, so we have to correct for natural silicon, using the data from their earlier paper which quotes results for all isotopes, but these are given as the $(2p_{3/2}\text{-}1s_{1/2})$ transition, so again have to be corrected. A similar tale of woe complicates the $(3p\text{-}1s)$ transition, except that this transition is given only in their earlier paper. For the higher transitions, they are taken from the publication of Schaller *et al.* [5], but their results for the $(2p\text{-}1s)$ and $(3p\text{-}1s)$ transitions are clearly about 70 eV lower than the results of Fricke, so we raise the Schaller values by this amount, and raise the error from 30 to 40 and 50 eV. This logic was also used in Table 3.4 of the review by Measday [4]. After all these corrections are applied, the agreement with our results is excellent, but of course we use the $(2p\text{-}1s)$ as a calibration point, so this may be a circular argument, except that the energies of the other x rays is really governed by the 511 keV calibration from annihilation radiation.

For the intensities, the comparison with Suzuki is straight forward [10], but Mausner *et al.* [47] give their results purely as a ratio viz. K_β/K_α , K_γ/K_α etc., so we had to add our value for the $[(7 \text{ to } \infty)p\text{-}1s]$ to obtain an overall normalization. Their results are slightly inconsistent with ours, but we note that Bergmann *et al.* [40] also obtained an accurate value of 9.23(25) for K_β/K_α, which agrees much better with our value of 9.22(34) than the value 8.2(3) of Mausner *et al.* We shall use our own values for the overall normalization of the muon capture γ rays, but the differences are not consequential.

We now discuss the various reactions for muon capture in natural silicon. We first note that we observe a few γ rays which come from the less abundant isotopes, viz. ^{29}Si (4.67%), and ^{30}Si (3.10%), see Table XIII. Most of these yields are marginal. For a few other γ rays in these nuclides, we could just place limits of about 0.2%.

We turn now to the principal isotope ^{28}Si, which has an abundance of 92.23%. For the reaction ^{28}Si$(\mu^-, \nu\gamma)^{28}$Al, we observe several very clear γ rays, see Table XIV. Previous results are compatible with ours on the whole, but several

TABLE XIII. Observed γ rays which come from muon capture in the less abundant isotopes of silicon, viz. ^{29}Si and ^{30}Si. The yield is that for natural silicon.

Nuclide	Level (keV)	J^π	Transition branching ratio (%)	Transition energy (keV)	Observed γ-ray yield (%)
^{30}Al	243.90	$(1^+, 2)$	100	243.89	0.4(2)
^{30}Al	687.53	1^+	50	443.62	0.4(4)[a]
			50	687.52	<0.04
^{29}Al	1398.0	$1/2^+$	100	1397.9	0.36(7)
^{29}Al	1754.2	$7/2^+$	100	1754.1	0.13(5)

[a]Probably another identification, yet unknown.

TABLE XII. The muonic Lyman (or K) series x rays for natural silicon, giving the observed energy and the absolute intensity per muon stop, normalized to 100% for the sum of this series. We compare to previous results for the energies [5–7], all corrected to be the result for the center of gravity for natural silicon. We also compare to previous values for the intensities [10,47].

μ x ray	Energy (keV) (this exp.)	Energy (keV) [5–7]	Intensity (%) (this exp.)	Intensity (%) [10]	Intensity (%) [47]
$2p\text{-}1s$	400.177[a]	400.177(5)	80.3(8)	79.2(22)	82.6(10)
$3p\text{-}1s$	476.80(5)	476.829(12)	7.40(20)	8.3(8)	6.8(3)
$4p\text{-}1s$	503.58(10)	503.59(4)	4.27(20)	3.3(6)	4.0(2)
$5p\text{-}1s$	515.97(10)	515.99(5)	3.83(20)	9.3(23)[b]	2.9(2)
$6p\text{-}1s$	522.74(10)	522.70(5)	2.29(10)	incl.[b]	1.8(1)
$(7 \text{ to } \infty)p\text{-}1s$			1.87(20)	incl.[b]	{1.9}[c]

[a]This energy was used in the calibration.
[b]The value of 9.3(23)% is for all higher transitions.
[c]This value was taken from our own data.

TABLE XIV. Observed γ-ray yields, per muon capture, for the reaction ^{28}Si(μ^-, $\nu\gamma$)^{28}Al, compared to the previous results of Miller *et al*. [18] and Gorringe *et al*. [19]. We have renormalized our results up by 3% to correct for the effect of the other isotopes of natural silicon.

Level in ^{28}Al (keV)	J^π	Transition branching ratio (%)	Transition energy (keV)	Observed γ-ray yield (%) (This exp.)	Observed γ-ray yield (%) [18]	Observed γ-ray yield (%) [19]
30.64	2^+	100	30.64	–	13.1(13)	15.8(19)
972.38	0^+	100	941.72	2.30(11)	2.0(3)	2.96(36)
1013.63	3^+	38	1013.61	0.18(18)[a]	–	–
		62	982.97	0.17(17)[a]	–	–
1372.95	1^+	4.7	1372.91	[a]	–	–
		55	1342.27	1.19(21)	1.7(2)	1.84(34)
		40	400.56	[a]	–	–
1620.32	1^+	6	1620.26	[a]	1.8(3)	$\sim$0
		92	1589.63	1.10(16)	1.7(3)	1.51(22)
1622.92	2^+	92.8	1622.86	0.55(33)	–	–
		7.2	1592.23	0.11(8)	–	–
2138.92	2^+	41	2138.83	0.85(21)	1.0(3)[b]	{2.63(38)}[c]
		52	2108.19	0.84(16)	1.5(3)[b]	{1.94(29)}[c]
		7	1125.26	0.13(7)	–	–
2201.46	1^+	79	2170.73	4.31(42)	4.6(3)	6.26(68)
		16	1229.05	0.76(13)	1.1(2)	1.06(20)
2271.77	4^+	100	2271.67	$<$0.11	–	–
2486.18	2^+	22	2486.06	$<$0.12	–	–
		61	865.84	0.10(5)	–	–
		11	863.24	0.02(5)	–	–
3105	$(1, 3)^+$	75	3074.1	0.84(8)	–	1.27(22)
		25[d]	903.5	$<$0.1	–	–
3541.9	1^+	100[e]	1918.91	0.15(11)	–	–
3875.78	2^-	79	3875.49	1.0(3)	–	0.84(27)
		15	2255.36	0.13(13)	–	–
4115	1^+	0.1[f]	4115	$<$0.2	–	–
		10[f]	4084	0.34(20)	–	–
		30[f]	2742	0.23(15)	–	–
		19[f]	2490	0.23(12)	–	–
		26[f]	1974	$<$0.1	–	–
4596.51	3^+	71	2973.42	$<$0.2	–	–
4848.73	1^+	72[f]	4818.09[g]	1.0(2)	–	–
(4843.62)[h]			(4812.54)[h]			
4996.92	2^-	54	4996.44	0.32(16)	–	–
		40	4965.81	$<$0.20	–	–
5442.28	2^-	59	5411.08	0.73(34)	–	–
		32	3303.15	0.66(15)	–	–
5741.12		96	5709.85	0.45(22)	–	–
6419.84	2^+	78	4280.56	0.32(32)	–	–
7725				$<$0.5	5.4(40)	–

[a]These lines are difficult to distinguish from their surroundings.
[b]Taken from Table VII of Miller's thesis [48].
[c]Their spectrum is contaminated in this region.
[d]This is the literature value [49]; we find $<$13%, and assume it to be zero in any calculation.
[e]This value comes from an earlier compendium and is thus suspect.
[f]There are no experimental values, so we use the calculations of Kuz'min and Tetereva [25].
[g]We find 4814(2).
[h]From Schmidt *et al*. [50], see text.

detailed comments need to be made. Unfortunately we kept our energy threshold around 120 keV, so did not observe the 30.6 keV transition, which is a key normalizing factor.

Overall the agreement between the three experiments is satisfactory, although our yields tend to be about 80% of those of Gorringe *et al*. [19]. We shall not discuss in detail an experiment by Pratt [51], which had fairly large errors and was earlier than that of Miller *et al*., but consistent. For those transitions detected by Gorringe *et al*., but not by Miller *et al*., viz. the levels at 3105 and 3876, we also detect them clearly, with compatible yields.

We identify some strength from the level at 1622.92 keV, although Gorringe *et al*. suggested that there was little strength for the 1622.86 keV transition. This is a complicated region as one would expect a yield of 0.06% for the (1620 g.s.) transition at 1620.26 keV, but worse still an unknown yield from the (1851–228) transition at 1622.26 keV from ^{26}Al. Miller *et al*. attributed the peak to ^{28}Al, and Gorringe *et al*. attributed it all to ^{26}Al. All the levels have a short lifetime (<100 fs) so are spread out over 12 keV by the Doppler shift. Thus we take an empirical approach and use the observed energy of 1622.46 keV to split the total yield of 1.65% in the ratio 2:1, i.e. 1.1% for the 1622.26 keV transition in ^{26}Al, and 0.55% for the 1622.86 transition in ^{28}Al, but have to concede large errors (±0.33) to this distribution because of the uncertainty in the energy calibration. In support of our hypothesis, we note that we might have observed the (1623 - 31) transition at 1592.23 keV with a yield of 0.11(8)%, a transition with a branching ratio of 7.2%, and we might also have detected transitions to this level, 0.07(7)% from the 2988 keV level, and 0.15(11)% from the 3542 keV level, but both are very marginal identifications. We shall also see that our yield for the ^{26}Al transition is somewhat higher than others to the same product nuclide.

In Fig. 5 we illustrate the spectrum from 1550 to 1750 keV, and the complexity of the lineshapes is obvious. At 1589 keV is the (1620 - 31) transition in ^{28}Al; the 1620 keV level supposedly has a lifetime of 85(40) fs, which means that some recoiling ions are slowing down, but the peak seems too narrow. At 1699 keV is a narrow line produced in the reaction ^{28}Si(μ^-, $\nu p\gamma$)^{27}Mg, which would normally broaden the line, but the level at 1699 keV has an unusually long lifetime of 0.98 ps, so most recoilling ions will stop. The broad line at 1720.3 keV is the (2735 - 1014) transition from the reaction ^{28}Si(μ^-, $\nu n\gamma$)^{27}Al, and the 2735 keV level has a short lifetime of 8.9 fs, so most ions decay in flight, and the width is caused by the effect of the recoil from the neutrino and then the neutron. Now we can consider the peak at 1622 keV, and it is clearly a mixture of lines, but because of the individual shape for each reaction, modified by the level lifetime, we hesitate to interpret its shape. To view simpler interpretations we can consider the next figure.

In Fig. 6 we illustrate the region around 2000 to 2300 keV. The peak at 2171 is from reaction ^{28}Si(μ^-, $\nu\gamma$)^{28}Al, and indicates the expected box-like structure for such a reaction, including a little smoothing of the edges due to resolution and also from slowing down of the recoil ion. Now the lifetime of the level at 2171 is 41(4) fs, which is shorter but not that much shorter than the supposed 85(40) fs of the 1620 keV level, shown in Fig. 5. Now the shape of that 1589 keV transition from the 1620 keV level is also very similar to that for the (1373 - 31) transition from a level with a lifetime of 220(35) fs (not illustrated), thus we suggest that the lifetime of the 1620 keV level is similar, viz. about 200 fs and not 85 fs.

Returning to Fig. 6, at 2211 keV is a typical neutron production shape from reaction ^{28}Si(μ^-, $\nu n\gamma$)^{27}Al, superimposed by the narrow neutron capture line on hydrogen at 2223 keV, which is a useful energy calibration, and also indicates the intrinsic resolution of the detector. The situation at 2108 and 2139 keV is more complex. They are transitions from the

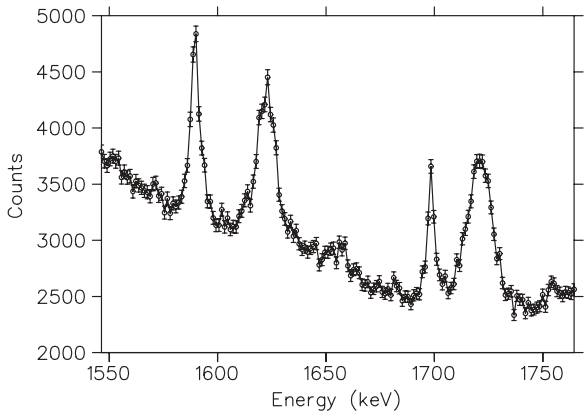

FIG. 5. A spectrum for muon capture in ^{28}Si, illustrating the complexity of the peak at 1622 keV. The peak at 1699 keV is from the reaction ^{28}Si(μ^-, $\nu p\gamma$)^{27}Mg, but the level lifetime is 0.98 ps, so the recoilling ion mostly stops, and the shape is close to the detector resolution. The broad triangle at 1720.3 keV is from the reaction ^{28}Si(μ^-, $\nu n\gamma$)^{27}Al. (We suggest that the lifetime of the 1620 keV level which produces the transition at 1589 keV is much longer than the literature value of 85(40) fs, probably about 200 fs).

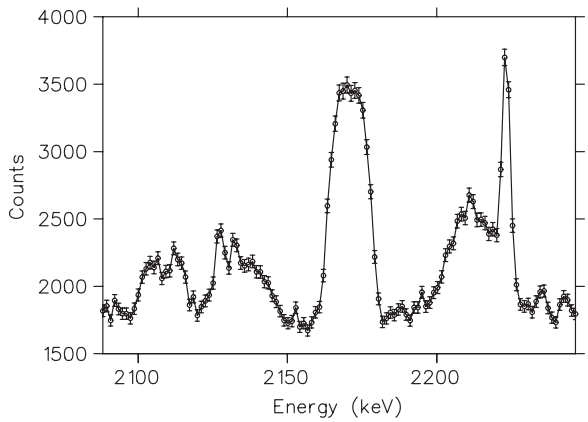

FIG. 6. The spectrum for muon capture in ^{28}Si showing a clean peak at 2171 keV from the reaction ^{28}Si(μ^-, $\nu\gamma$)^{28}Al, Doppler broadened in a box-like manner. At 2108 and 2139 keV are two other structures from the reaction ^{28}Si(μ^-, $\nu\gamma$)^{28}Al, also Doppler broadened in a box-like manner, but clearly contaminated. In addition there is the 2223 keV line from ($np \rightarrow \gamma d$), superimposed on the 2211 keV line from the reaction ^{28}Si(μ^-, $\nu n\gamma$)^{27}Al. These yields can be separated quite confidently.

reaction ^{28}Si(μ^-, $\nu\gamma$)^{28}Al, being the 31 keV and ground state transitions from the 2139 keV level, and should have the relative branching ratio 52:41, and also should have the same width and shape as the peak at 2171 keV. Clearly the peak at 2139 keV is too broad and has unexpected structure which we attribute to six lines, the major ones being at 2127 keV from ^{34}S (from muon capture on ^{35}Cl) and at 2133 keV from ^{26}Mg; even the 2108 keV box seems to have a little contamination. Our results are compared in Table XIV with those of Gorringe *et al*. [19]. Ours are significantly smaller than theirs, but even visually one can see that the 2108 peak has a yield about 1/5 of that of the 2171 keV box, and this is not true for the yields of Gorringe *et al*. Thus we believe our values are more reasonable.

The level at 3105 keV is interesting because the literature gives two transitions leaving the level; this is from an early experiment by Lawergren and Beyea [49] who found the ground state transition to have a branching ratio of 75(7)%, and a transition to the 2201 keV level (with an energy of 903.5(10) keV) to have a branching ratio of 25(3)%. No evidence is presented except an entry in their Table III. We observe no 903.5 keV transition, and can place a limit of $<$13% on the branching ratio. In our earlier experiment on ^{28}Si, for which this transition would have been a catastrophe, a careful analysis was made; a limit of $<$12% was placed using a co-incidence technique [31], and a limit of $<$7% using the singles spectrum [30]. We conclude that there is no evidence for the transition (3105 - 2201) at 903.5 keV and henceforth assume it to be zero. We also note that Kuz'min and Tetereva calculate that this branching ratio is very small (0.1%). A further complication is that Schmidt *et al*. [50] in their experiment on the reaction ^{27}Al(n, γ)^{28}Al do not list the 3105 keV level, nor the 903.5 keV γ ray, but do mention an unidentified transition at 3075.65(9) keV, and if this is the transition through the 30.6 keV level, this puts the 3105 level at 3106.4 keV (with a 0.2 keV recoil correction). Our energy calibration is not secure enough to distinguish these values of the transition energy, though for what it is worth, we obtain 3076.5(20). This level probably has a J^π of 1^+, and it is not surprising that it is weakly excited in the (n, γ) reaction. Vernotte *et al*. [52] prefer 1^+, not 3^+ for this level, in their study of the reaction ^{29}Si(d,^{3}He)^{28}Al, which is compatible with our detecting some yield. They also prefer 3^+ for the 4596.5 keV level, which is compatible with our non-observation of a yield.

Another 1^+ level is at 4115 keV, and Kuz'min and Tetereva [25] suggest fairly strong feeding in the (μ^-, $\nu\gamma$) reaction; the level is poorly established, and no experimental branching ratios are available. The calculation of Kuz'min and Tetereva agree quite well with experimental values for the γ-ray branching ratios for the 1^+ levels, as noted above, contradicting the then existing experimental values for the 3105 keV level, but in agreement with our observations; similarly they obtain very low branching ratios for the ground state transitions of the 4115 and 4848 keV levels, similar to our own observations. Thus we take their values for the 4115 and 4848 keV levels, but emphasize that our observations for the 4115 transitions are all very marginal, and could easily be contaminated by unknown γ rays. Just adding the observed yields we obtain a direct yield of 0.85(30)%, in excellent agreement with the capture calculations of Kuz'min and Tetereva [25], which gave 0.97%.

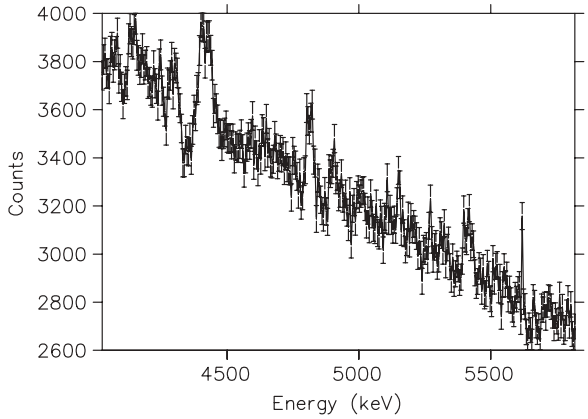

FIG. 7. The spectrum for muon capture in ^{28}Si at high energy. The peak at 4420 keV is a mixture of the Doppler broadened line at 4410 keV from ^{27}Al, mixed with the ^{12}C(n, n') line at 4438 keV. The box at 4814 keV is attributed to a new line in ^{28}Al, and another box at 5411 is also attributed to ^{28}Al, being the transition (5442 - 31). There is a narrow line at 5618 keV from the single escape of the 6129 keV line from ^{16}N β decay from activated water.

We illustrate in Fig. 7 the high energy region from 4 to 6 MeV. Strong box-like γ rays are observed at 4814 and 5411 keV indicating an origin from the reaction ^{28}Si(μ^-, $\nu\gamma$)^{28}Al; in addition there is a doublet at 4420 keV coming from a γ ray from ^{27}Al at 4410 keV, and the well known background γ ray from ^{12}C(n, n') at 4438 keV. The narrow peak at 5618 keV is the single escape of the line at 6129 keV which comes from ^{16}N beta decay, an activity produced aplenty from the reaction ^{16}O(n, p)^{16}N in the cooling water of magnets. This peak indicates the intrinsic resolution of the HPGe detector, and is a good energy calibration.

This transition at 4814(2) keV, is probably from a 1^+ level feeding through the first excited state at 30.64 keV. This level has a mottled history; Schmidt *et al*. detected a γ ray at 4812.54(17) keV, which would put the level at 4843.62 keV, if it were a cascade through the first excited state at 30.64 keV, but did not put it in the level scheme themselves. Endt first took a fairly noncommittal stance [53], but later revised these identifications [54] (see footnote to Table 28c), and the new compendium follows his most recent recommendation, proposing a level at 4848.73(1), yet no γ ray transitions are recommended. We prefer the other identification for the 4812.54 keV line, as we see a strong γ ray at 4814(2) keV with a yield of 1.0(2)%. We note that Gorringe *et al*. also detected a γ ray at 4815 keV from muon capture in silicon, but decided not to pursue its identification. However, because of the width of these lines, and the poor statistics, neither experiment is sufficiently secure in its energy calibration to clearly distinguish between these two alternatives.

We have searched for other high energy γ rays in ^{28}Al up to 7.7 MeV. There are many levels, but most do not have a specified spin and parity, nor γ-ray branching ratios. For the few which have such branching ratios we find none at a level

TABLE XV. Deduced values for the direct excitation of levels from the reaction ^{28}Si(μ^-, ν)^{28}Al, taking account of the transition branching ratios and known cascading from Table XIV. We compare with results of the reaction ^{28}Si(π^-, γ)^{28}Al [23], normalized to our value for the 2201 keV level. We also list the results of the muon capture calculation for the 1^+ levels by Kuz'min and Tetereva [25].

Level in ^{28}Al (keV)	Known cascading (%)	Direct yield per muon capture (%)	^{28}Si(π^-, γ)^{28}Al experiment [23]	Theory [25]
0	16.6(12)	–	sum	–
30.64	11.0(6)	3.4(13)	is 1.9	–
972.38	1.78(16)	0.5(2)	sum	–
1013.63	0.12(2)	0.25(18)	is 3.0	–
1372.95	0.03(2)	2.1(4)	1.4	1.48
1620.32	–	1.20(17)	–	0.87
1622.92	0.22(13)	0.74(46)	–	–
2138.92	0.92(40)	0.86(50)	–	–
2201.46	–	5.28(45)	5.3	7.32
2271.77	–	<0.11	–	–
2486.18	–	<0.5	–	–
3105	–	0.84(8)	1.5	1.29
3541.9	–	0.15(11)	0.4	∼0
3875.78	–	1.25(38)	sum	–
4115	–	0.85(30)	is 3.3	0.97
4848.73	–	1.0(2)	sum	2.15
4996.92	–	0.46(23)	of	–
∼5017	–	no clear ID	all	0.84
∼5435	–	no clear ID	five	0.76
5442.28	–	1.9(4)	is 5.1	–
5741.12	–	0.45(22)	sum of	–
∼5919	–	no clear ID	all three	0.48
6419.84	–	0.4(4)	is 12.1	–

TABLE XVI. Observed γ-ray yields, per muon capture, for the reaction ^{28}Si(μ^-, $\nu n\gamma$)^{27}Al, compared to the previous results of Miller *et al.* [18]. We have raised our observed yields for natural silicon by 8.4% to obtain the yield for ^{28}Si.

Level in ^{27}Al (keV)	J^π	Transition branching ratio (%)	Transition energy (keV)	Observed γ-ray yield (%) (This exp.)	Observed γ-ray yield (%) [18]
843.76	$1/2^+$	100	843.74	9.9(10)	11.4(8)
1014.45	$3/2^+$	97	1014.42	9.21(13)	10.3(8)
2211.1	$7/2^+$	100	2211.0	2.6(4)	1.8(10)
2734.9	$5/2^+$	22	2734.7	0.90(9)	–
		76	1720.3	2.46(28)	0.8(7)
2982.00	$3/2^+$	97	2981.82	2.2(5)	2.6(8)
3004.2	$9/2^+$	89	3004.0	0.6(3)	–
3680.4	$1/2^+$	61	2836.4	0.83(11)	0.6(2)
		38	2665.8	0.36(17)	–
3956.8	$3/2^+$	85	3956.4	1.2(3)	–
4054.6	$1/2^-$	86	3210.6	1.7(2)	–
		14	3039.9	0.24(22)	–
4410.2	$5/2^+$	58	4409.8[a]	0.8(4)[a]	–
		35	3395.5	0.42(15)	–
4510.3	$11/2^+$	77	2299.0	0.08(8)	–
4580.0	$7/2^+$	70	4579.5	0.3(3)	–
4811.6	$5/2^+$	45	3796.8	<0.3	–
5155.6	$3/2^-$	80	5155.0	0.6(2)[b]	–
		20	4140.8	0.7(1)[b]	–
5432.8	7/2	44	5432.2	0.2(2)	–
		39	2428.4	0.1(1)	–

[a]This γ ray is very close to the 4438 keV line from ^{12}C.
[b]Inconsistent with literature branching ratios. We assume the 4140.8 keV line is contaminated.

of 0.5%. Even if no values were in the compilation, we would observe it if it were above 1%, but we do not observe any unknown γ rays at this yield.

Finally we note that Miller *et al.* claim a γ ray at 7725 keV in ^{28}Al with a yield of $5.4 \pm 40\%$, a strange number, but one which is also found in Table VII, p. 176, of Miller's thesis [48]. Assuming this is not a typographical error, we identify it as a background line from ^{27}Al(n, γ)^{28}Al, which Schmidt *et al.* give as 7724.036(4) keV [50]. We place a limit on the equivalent yield of <0.5% from our own spectrum, assuming it is a line broadened to ∼60 keV). For the real (n, γ) line, it would be ∼10 keV wide (our resolution),and our limit is then lowered to even less, <0.2%. Note that for background lines like this, their apparent yield depends on the thermal neutron flux in the experimental area, on timing cuts, and on the material around the detector. This all varies enormously from one experiment to another.

We now present in Table XV the direct excitation of these levels in ^{28}Al, taking into account the branching ratios and the cascading. We compare with the experiment on the reaction ^{28}Si(π^-, γ)^{28}Al [23], for which we have arbitrarily normalized their results to 5.3 for the 2201 transition, in order to make the comparison easier. The correlation is remarkably good considering that the π^- is absorbed from the $2p$ level, not the $1s$ as is the case for the μ^-. The only major discrepancy is the strength they observe at around 6.1 MeV, and as ^{28}Al is bound up to 7724 keV, all of this should be detected by us. There is confirming evidence that we are missing strength in that two activation experiments agree that the reaction ^{28}Si(μ^-, ν)^{28}Al is much stronger than we observe; Miller *et al.* [18] found 26(3)% and Bunatyan *et al.* [55] found 28(4)% for the sum of all transitions. Note that the authors of the experiment on the reaction ^{28}Si(π^-, γ)^{28}Al attribute the higher excitation peaks at 4.1, 5.2, and 6.1 MeV to 2^- transitions which had been identified as $T = 1$ levels in inelastic electron scattering off ^{28}Si at 180° [56]. However it is clear that each of the (π^-, γ) peaks corresponds to at least three levels each, most of which are 2^- but some are 1^+. We also compare to the calculation by Kuz'min and Tetereva [25] for the 1^+ levels, and again obtain reasonable agreement. Unfortunately they did not calculate the yields for the 2^- levels.

We turn now to the reaction ^{28}Si(μ^-, $\nu n\gamma$)^{27}Al, which is observed to be quite strong, as expected, see Table XVI. We have raised our yields for natural silicon by 8.4% to account for the heavier isotopes which would not produce ^{27}Al in any quantity. We have also corrected the yields of the 844 and 1014 keV lines which have a contribution of about 1.5% and 1.1%, respectively, from background caused by the reaction ^{27}Al(n, n')^{27}Al in structural aluminum. We compare with the results of Miller *et al.* [18], who used an enriched target. The

TABLE XVII. Deduced values for the direct excitation of levels from the reaction ^{28}Si(μ^-, νn)^{27}Al, taking account of the transition branching ratios and known cascading from Table XVI. We compare with the integrated cross sections for the (γ, p) reaction from Thomson and Thompson [28] and from Gulbranson [27], (correlation coefficient $r = 0.95$) and spectroscopic factors from the reaction ^{28}Si(d,^{3}He)^{27}Al [26] ($r = 0.76$).

Level in ^{27}Al (keV)	Known cascading (%)	Direct yield per muon capture (%)	$\sigma(\gamma, p)$ reaction [28]	$\sigma(\gamma, p)$ reaction [27]	(d,^{3}He) reaction [26]
0	28(2)	{19}[a]	24	21.8	4.6
843.76	2.5(2)	7.4(10)	15	10.0	1.2
1014.45	4.1(3)	5.1(3)	8	4.1	1.0
2211.1	0.2(2)	2.4(4)	<1	0.8	<0.3
2734.9	–	3.7(3)	6	2.5	0.9
2982.00	–	2.3(5)	5	sum is	0.9
3004.2	0.02(2)	0.7(3)	–	2.6	<0.06
3680.4	0.13(13)	1.2(2)	3	1.1	0.1
3956.8	–	1.4(4)	–	sum is	small
4054.6	–	2.0(2)	4	2.4	2.9
4410.2	–	1.3(4)	v. small	0.6	0.8
4510.3	–	0.1(1)	–	–	–
4580.0	–	0.4(4)	–	–	–
4811.6	–	0	–	–	–
5155.6	–	0.63(25)	–	~3[b]	2.3
5432.8	–	0.34(34)	–	–	–

[a]Estimate from the comparison reactions.
[b]Estimate from Fig. 4 of Gulbranson *et al.* [27].

agreement is excellent. Note that our values for the transitions from the 5155.6 keV level are inconsistent; this transition is expected, but we take the ground state transition to be definitive, and assume that the 4141 keV transition is contaminated with an unidentified γ ray. We also searched for fifteen transitions from levels higher in energy than the 5432.8 keV level, and could place limits on the yield for each of about <0.4%.

We can now obtain the direct production of these levels by taking account of the branching ratios, and subtracting off the cascading, see Table XVII. We compare with (a) the reaction ^{28}Si(γ, p)^{27}Al studied by Thomson and Thompson [28] using γ-ray detection for a 28 MeV bremsstrahlung beam, (b) the reaction ^{28}Si(γ, p)^{27}Al studied by Gulbranson *et al.* [27] who integrated their proton detection experiment from 15.6 to 22.5 MeV, and (c) the reaction ^{28}Si(d,^{3}He)^{27}Al using an average value of the spectroscopic factors given in the compendium of Endt and van der Leun [26].

As was found by Miller *et al.* [18], the comparison with the reaction ^{28}Si(d,^{3}He)^{27}Al is useful, but a better correlation is with the (γ, p) reaction. If we take the first four excited states, plus the levels at 3680 and 4410 MeV, then we obtain a correlation coefficient of $r = 0.95$ between our data and the (γ, p) results of Gulbranson [27], but $r = 0.76$ for the spectroscopic factors. Note that the level at 3004 keV is excited quite strongly in the reaction ^{28}Si(d,^{3}He)^{27}Al, notwithstanding the low spectroscopic factor, but the transition does not

TABLE XVIII. Observed γ-ray yields, per muon capture, for the reaction ^{28}Si(μ^-, $\nu 2n\gamma$)^{26}Al, compared to the previous results of Miller *et al.* [18]. We have raised our observed yields for natural silicon by 8.4% to obtain the yield for ^{28}Si.

Level in ^{26}Al (keV)	J^π	Transition branching ratio (%)	Transition energy (keV)	Observed γ-ray yield (%) (This exp.)	Observed γ-ray yield (%) [18]
228.30	0^+	β^+	228.30	<0.04	0.7(2)
416.85	3^+	100	416.85	0.9(2)	0.9(2)
1057.74	1^+	100	829.42	0.65(22)	–
1759.03	2^+	98	1342.15	0.15(15)	–
1850.62	1^+	99	1622.26	1.16(36)[a]	–
2068.86	4^+	31	2068.77	<0.13	–
		69	1651.95	<0.26	–
2069.47	2^+	21	1652.56	<0.26	–
		75	1011.71	<0.38	–
2071.64	1^+	89	1843.26	0.14(7)	–

[a]Mixed with the 1622.86 keV transition from ^{28}Al, see text.

have a simple interpretation. From these comparisons, we estimate that the direct ground state transition for the reaction ^{28}Si(μ^-, νn)^{27}Al is about 19%, which, with the observed γ rays, gives a total for this reaction of 47%.

We now turn to the reaction ^{28}Si(μ^-, $\nu 2n\gamma$)^{26}Al which is clearly detected, but has a low yield, see Table XVIII. The comparison with Miller *et al.* is perfect for the 417 keV transition, but they claimed to observe the ^{26}Al transition at 228 keV. This level decays by β^+ emission, not by a γ ray, so nothing is to be expected, in agreement with our data. We assume that they were detecting a nearby background line. Note that the yield of the 1622 keV transition is somewhat higher than others around it; remember that this region is a confusion of three lines, two from ^{28}Al at 1620.26 and 1622.86, and this one from ^{26}Al at 1622.26; we discussed this above and attribute the yield according to the observed energy, taking the 1620.26 contribution to be 0.06%.

There is little cascading; the 1759 level cascades through the 417 keV line, contributing 0.15(15)% to the observed yield; all other γ rays go to the ground state or the 228 keV first excited state, which we should not detect. In a study of the (π^-, $2n$) reaction, Zaider *et al.* [17] detected the 417 keV transition, but placed only a limit on the 829 keV transition which was about half of that for the 417 keV transition, just about compatible with our results. A more interesting comparison is with the reaction ^{28}Si(d, α)^{26}Al, and this is presented in Table XIX.

The two studies of the reaction ^{28}Si(d, α)^{26}Al give rather different relative yields, which is not surprising as the deuteron energies are very different. The older result of Browne [56] was for 7 MeV deuterons, and the α particles were observed at 60°, whereas the more recent experiment by Takahashi *et al.* [29] used 33 MeV deuterons and the α spectrum was taken at 12°. You would not expect the (d, α) reaction to feed the 228 keV level strongly, because it is $T = 1$, although isospin violating reactions do occur at such energies [58]. The comparison with muon capture is confusing, but it does enable us to estimate the ground state yield in muon capture; it also indicates that the

TABLE XIX. Deduced values for the direct excitation of levels from the reaction ^{28}Si(μ^-, $\nu 2n$)^{26}Al, taking account of the transition branching ratios and known cascading from Table XVIII. We compare with results of the the reaction ^{28}Si(d, α)^{26}Al by Takahashi *et al.* [29], and by Browne [57], normalized to the ground state transition.

Level in ^{26}Al (keV)	Known cascading (%)	Direct yield per muon capture (%)	Yield for ^{28}Si(d, α)^{26}Al [29]	Yield for ^{28}Si(d, α)^{26}Al [56]
0	2.8[a]	1.0(3)[b]	100	100
228.30	1.9(4)	n.a.	0	8
416 85	0.15(15)	0.75(25)	87	68
1057.74	–	0.65(22)	16	62
1759.03	–	0.15(15)	3	57
1850.62	–	1.2(4)	16	14
2068.86	–	<0.4	sum	sum
2069.47	–	<0.5	is	is
2071.64	–	0.16(8)	13	157

[a]This is the sum of all direct feeding; in fact cascading through the 228 keV level is lost to beta decay.
[b]Estimate from the (d, α) reaction.

1851 keV level, originator of the 1622 keV transition, is not special, and so the attributed yield in muon capture is probably too high.

We have searched for transitions from the reaction ^{28}Si(μ^-, $\nu 3n\gamma$)^{25}Al but observed nothing, placing limits of <0.1% on the most likely. In contrast to ^{27}Al, we observe proton production reactions quite strongly in ^{28}Si. In Table XX we present our results for the reaction ^{28}Si(μ^-, $\nu p\gamma$)^{27}Mg, comparing with the one result from Miller *et al.* [18]. The agreement is satisfactory, but we observe many more γ rays.

The reaction ^{28}Si(μ^-, $\nu pn\gamma$)^{26}Mg is observed very clearly, see Table XXI. We detect a total direct yield of 8.4(8)%.

We even detect the reaction ^{28}Si(μ^-, $\nu p2n\gamma$)^{25}Mg, albeit rather weakly, see Table XXII, obtaining a total yield for γ rays of 1.5(1)%. For the reaction ^{28}Si(μ^-, $\nu p3n\gamma$)^{24}Mg, we detect the transitions at 1368.63 and at 2754.01 keV each with a yield of about 0.5%, but they are also produced from ^{24}Na decay, which is detected in background runs, so we attribute most of these γ rays to this background.

TABLE XX. Observed γ-ray yields, per muon capture, for the reaction ^{28}Si(μ^-, $\nu p\gamma$)^{27}Mg compared to the previous result of Miller *et al.* [18]. We present our observed yields for natural silicon because the isotope ^{29}Si probably contributes more than in proportion to its abundance. The transition energies have been calculated from the newly recommended values for the level energies [14].

Level in ^{27}Mg (keV)	J^π	Transition branching ratio (%)	Transition energy (keV)	Observed γ-ray yield (%) (This exp.)	Observed γ-ray yield (%) [18]
984.92	$3/2^+$	100	984.90	1.41(34)	1.9(2)
1698.63	$5/2^+$	100	1698.57	0.62(12)	–
1940.35	$5/2^+$	33	1940.28	0.23(6)	–
		66	955.41	0.22(4)	–
3109.4	$(3/2, 7/2)^+$	87	1169.0	0.14(7)[a]	–

[a]May be contaminated by Mn muonic x rays.

TABLE XXI. Observed γ-ray yields, per muon capture, for the reaction ^{28}Si(μ^-, $\nu pn\gamma$)^{26}Mg compared to the previous results of Miller *et al.* [18]. We have raised our observed yields for natural silicon by 8.4%.

Level in ^{26}Mg (keV)	J^π	Transition branching ratio (%)	Transition energy (keV)	Observed γ-ray yield (%) (This exp.)	Observed γ-ray yield (%) [18]
1808.73	2^+	100	1808.66	7.9(8)	10(1)
2938.34	2^+	90	1129.58	2.11(14	3.2(5)
		10	2938.16	0.52(23)	–
3588.56	0^+	100	1779.77	<2.0[a]	–
3941.55	3^+	38	2132.73	0.14(7)	–
		62	1003.19	0.25(5)	0.09(6)
4318.88	4^+	100	2510.02	0.49(24)	–
4332.57	2^+	79	2523.71	<0.13	–

[a]Drowned by the 1778.97 keV transition from ^{28}Si itself, mostly from ^{28}Al decay.

For the reaction ^{28}Si(μ^-, $\nu\alpha\gamma$)^{24}Na, we detect the 472.21 keV line but this is also produced by the background reaction ^{23}Na(n, γ)^{24}Na, and anyway this level has a lifetime of 20.2 ms, which means that it is impossible to estimate any yield. For the reaction ^{28}Si(μ^-, $\nu\alpha n\gamma$)^{23}Na, we detect the 439.99 keV transition, but this is also produced by a background reaction, viz. ^{23}Na(n, n')^{23}Na. We estimate that about half of this γ ray is background leaving 0.5(5)% as coming from muon capture. Higher transitions are not observed.

We can now consolidate our data for ^{28}Si into a summary table, giving the total yields, see Table XXIII.

There are several important constraints, other than our own data. First there are two measurements for the total production of ^{28}Al; Miller *et al.* obtained 26(3)%, and

TABLE XXII. Observed γ-ray yields, per muon capture, for the reaction ^{28}Si(μ^-, $\nu p2n\gamma$)^{25}Mg compared to the previous results of Miller *et al.* [18]. We have raised our observed yields for natural silicon by 8.4%. The transition energies have been calculated from the newly recommended values for the level energies.

Level in ^{25}Mg (keV)	J^π	Transition branching ratio (%)	Transition energy (keV)	Observed γ-ray yield (%) (This exp.)	Observed γ-ray yield (%) [18]
585.09	$1/2^+$	100	585.08	1.00(8)	0.6(3)
974.85	$3/2^+$	51	974.83	0.30(6)	0.8(3)
		49	389.76	0.22(6)	–
1611.77	$7/2^+$	100	1611.71	0.07(7)	0.9(5)
1964.61	$5/2^+$	26	1964.53	0.04(4)	–
		47	1379.48	0.04(4)	–
		27	989.74	0.06(6)	–
2563.44	$1/2^+$	80	1978.7	<0.1	–

TABLE XXIII. Summary of the yield (in %) of all major muon capture reactions in ^{28}Si.

Reaction	Observed γ ray yield	Estimated ground-state transition	Missing yields	Total yield
^{28}Si$(\mu^-, \nu)^{28}$Al	16.6(12)	0.4	9	26
^{28}Si$(\mu^-, \nu n)^{27}$Al	28(2)	19	2	49
^{28}Si$(\mu^-, \nu 2n)^{26}$Al	2.8(5)	1	2.2	6
^{28}Si$(\mu^-, \nu 3n)^{25}$Al	$<$0.5	1	–	1
^{28}Si$(\mu^-, \nu p)^{27}$Mg	2.5(4)	0.5	–	3
^{28}Si$(\mu^-, \nu pn)^{26}$Mg	8.4(8)	2	$-$1.4	9
^{28}Si$(\mu^-, \nu p2n)^{25}$Mg	1.5(1)	1	–	2.5
^{28}Si$(\mu^-, \nu p3n)^{24}$Mg	$<$0.5	0.5	–	0.5
^{28}Si$(\mu^-, \nu\alpha)^{24}$Na	0.5(5)	0.5	–	1
^{28}Si$(\mu^-, \nu\alpha n)^{23}$Na	0.5(5)	0.5	1	2
Total	60.8	26.4	12.8	100

Bunatyan *et al*. [55] obtained 28(4)%. We have used 26% because it is hard to explain such a large missing yield for the reaction ^{28}Si$(\mu^-, \nu\gamma)^{28}$Al. Secondly there is the experiment by Sobottka and Wills [20], who stopped muons in a silicon detector and found that 15(2)% of captures yielded charged particles; this is hard to make consistent with our own results as we observe 13.4% from γ ray yields alone, and Miller *et al*. obtained an even higher number, so we use a total charge particle yield of 18%. Note that the values in Table XXIII are marginally different from Table 5.5 of the review [4], but very similar in the overall picture.

The values for ^{28}Si are somewhat different from those for ^{27}Al in Table XI. For capture in ^{27}Al, the (μ^-, ν) reaction is weaker as are the proton production reactions, but the reaction $(\mu^-, \nu n)$ and all the neutron production reactions are stronger; this is obviously just due to the neutron excess in ^{27}Al.

VI. OVERALL EXCITATION FUNCTION

We may now make some general comments about the neutrino spectrum from muon capture. We shall use the (π^-, γ) reaction for capture at rest as an experimental guide [59,60] because of the many similarities to muon capture, such as the mass of the initiating particle, and the excitation mechanism, which emphasizes unnatural parity levels, especially 1^+ and 2^-. We also have guidance from several similar reactions such as (p, n) and $(d, ^2\text{He})$ at forward angles, and (e, e') at 180° for electron energies around 60 MeV.

What is observed in the (π^-, γ) reaction is a clear excitation of bound states in the $(Z-1)$, A nucleus, but a stronger excitation of higher levels in the region of the giant dipole resonance (GDR). These are actually mainly 1^- spin-isospin levels, but are at a similar energy to the familiar GDR. (For muon capture, both the isospin and the spin-isospin 1^- modes are excited.)

The excitation in the (π^-, γ) reaction peaks around 20 MeV, but continues up to 30, 40, and even 50 MeV. This higher energy excitation was often described by a "pole term," i.e., a quasifree reaction on a nuclear proton, with subsequent emission of a free neutron. However the distinction between the pole term and giant resonance excitation remains unclear, even today.

Now for muon capture, one difference is that all the capture occurs from the $1s$ muonic level, whereas pion capture occurs mostly in the $2p$ orbit, but this makes surprisingly little difference. Secondly the muon mass is 35 MeV smaller, so the recoiling neutron is less energetic, and the importance of the pole term is reduced. Thirdly the muon capture operators are slightly different, permitting some $E1$ transitions.

To describe muon capture, we include our previous data for iodine and bismuth [3]. It is known that the average excitation energy varies little between light elements (18.0 MeV), and heavy elements (16.5 MeV) [61]. We also need information from photonuclear reactions, such as (γ, n), $(\gamma, 2n)$, and $(\gamma, 3n)$ [62]. Of course, there are normally no data for the product nucleus in muon capture, but we need only the general features. Thus for light elements, the $(\gamma, 2n)$ reaction takes 10 to 15 MeV above its threshold to become comparable to the (γ, n) reaction. However by mass 100, and for heavier nuclei, the $(\gamma, 2n)$ reaction rises quickly from threshold and within a few MeV has a larger cross section than the (γ, n) reaction. The $(\gamma, 3n)$ cross section rises a little more slowly and is not as dominant. We now add the information that fast neutron production in muon capture has been observed. Thus the yields for fast neutrons above 10 MeV in energy, per captured muon, are O, 26(5)%; Si, 17(2)%; Ca, 11(1)%; Pb, 11(2)%; see Table 4.11 in the muon capture review [4]. These neutrons come from low multiplicity modes at high excitation energy, a sort of pole term.

Thus we deduce that about 50% of the excitation in muon capture is above 15 MeV, 30% is above 20 MeV, and above 35 MeV there is still about 6%. Of course specific nuclides will vary a little from these average values. The excitation yields for the (π^-, γ) reaction are slightly higher as expected, 68(10)% above 15 MeV, 52(6)% above 20 MeV, and 16(3)% above 35 MeV, where the numbers in parentheses represents the variation between the sample nuclides of ^{24}Mg and ^{40}Ca [59].

Now for ^{27}Mg and ^{28}Al, the $(\gamma, 2n)$ thresholds are at 17.5 and 20.8 MeV, respectively, thus the observed $2n$ production in muon capture on ^{27}Al and ^{28}Si of 18% and 7% is less than expected, because much of this excitation is going to single

neutron emission. Similarly the $(\gamma, 3n)$ thresholds are at 24.9 and 32.1 MeV, respectively, a difference which explains the fact that the $3n$ yield in ^{28}Si is much less that in ^{27}Al, and again the lower multiplicity neutron production is taking some strength too.

We may also compare with muon capture calculations. There are many to choose from, but few actually display the excitation spectrum. We choose two examples; first the shell model calculation of Kolbe *et al*., for ^{40}Ca [63]. Their spectrum cuts off at 35 MeV, but if we take our own value of 6% excitation above 35 MeV, (their number would be almost certainly much smaller), then they obtain 44% excitation above 15 MeV, and 23% above 20 MeV. Thus they somewhat underestimate the higher excitation energies. For the phenomenological model of Hadermann and Junker [64], tuned specifically to give the neutron yields, they obtain an excitation of 56% above 15 MeV, 27% above 20 MeV, and 0.5% above 30 MeV. Thus we agree with their numbers around 10 to 20 MeV, but they severely underestimate the very high energies (>30 MeV), as they themselves note several times. Thus overall we believe that our various yields for the neutron production reactions have helped to consolidate the information on the excitation spectrum in muon capture.

VII. SUMMARY AND CONCLUSIONS

Our results for ^{27}Al and for natural silicon have slightly improved the results for the muonic Lyman x rays, and have greatly expanded the information for muon capture. For the muonic x rays, we reproduce the energies measured in previous experiments, which gives us confidence in our energy calibrations, and thus the identification of γ rays from muon capture. For the x-ray intensities, our results are in good agreement with the excellent study of Hartmann *et al*. for aluminum [8], and with that of Suzuki for silicon [10].

For muon capture, we have documented results for the first time for ^{27}Al. For silicon, we have observed more γ-ray transitions than had been identified before, in particular for the reaction $^{28}\mathrm{Si}(\mu^-, \nu)^{28}\mathrm{Al}$, we have detected several γ-rays in the 4 to 5 MeV region, confirming the importance of this region as seen in comparison reactions, and also in the calculations of Kuz'min and Tetereva [25]. For both ^{27}Al and ^{28}Si, we have observed many γ rays from the $(\mu^-, \nu n\gamma)$ reaction, and confirmed, yet again, that the feeding of the excited states correlates well with the (γ, p) reaction, though there are similarities with spectroscopic factors obtained from the $(d, ^3\mathrm{He})$ reaction too.

Two minor errors have been unearthed in the NNDC data compilation for ^{28}Al. For the 3105 keV level, we observe no transition to the 2201 keV level (<7%), whereas the data compilation gives 25(3)% from a single experiment in 1972. Similarly our spectrum for the 1589.6 keV γ ray from the 1620.3 keV level indicates little Doppler broadening. We suggest that the lifetime of this level is ~200 fs, not the value of 85(40) fs given in the data compilation.

We have identified hundreds of γ rays in our spectra, but a few (surprisingly few) remain unidentified, even some quite clear lines. Thus in the aluminum spectrum we detect unknown lines at 670, 786.70(7), 911, and 2154 keV, and in the silicon spectrum we observe unknown lines at 563, 670, 787, 929, and 1205 keV.

To progress further with muon capture in these elements will be difficult. Not only would the experimental spectra need much higher statistics, but studies of background lines would need to match any increased sensitivity. Perhaps more important, however, is that we were already limited by present knowledge concerning energy levels and transition branching ratios. Thus there is still a need for expansion of the general data base of nuclear properties.

ACKNOWLEDGMENTS

We wish to thank the many people who contributed to the successful completion of this experiment. E. Gete, T. P. Gorringe, J. Lange, and M. A. Saliba who helped set up the original experiment on nitrogen, and took some shifts too. J. Chuma wrote the program "PHYSICA" which was used for the data analysis, and also wrote some of the macros specifically for this analysis. Of course in a major laboratory like TRIUMF, many people help by keeping the cyclotron operating and preparing the experimental area for each experiment; the financial contribution for this essential activity is provided by the National Research Council of Canada. Finally we thank the Natural Sciences and Engineering Research Council, Canada, for providing grant OGP0090780 and 240164-01 that made the experiment possible.

[1] T. J. Stocki, D. F. Measday, E. Gete, M. A. Saliba, B. A. Moftah, and T. P. Gorringe, Nucl. Phys. **A697**, 55 (2002).
[2] D. F. Measday and T. J. Stocki, Phys. Rev. C **73**, 045501 (2006).
[3] D. F. Measday, T. J. Stocki, and H. Tam, Phys. Rev. C **75**, 045501 (2007).
[4] D. F. Measday, Phys. Rep. **354**, 243 (2001).
[5] L. A. Schaller, T. Dubler, K. Kaeser, G. Rinker, Jr., B. Robert-Tissot, L. Schellenberg, and H. Schneuwly, Nucl. Phys. **A300**, 225 (1978).
[6] G. Fricke, J. Herberz, Th. Hennemann, G. Mallot, L. A. Schaller, L. Schellenberg, C. Piller, and R. Jacot-Guillarmod, Phys. Rev. C **45**, 80 (1992).
[7] G. Fricke, C. Bernhardt, K. Heilig, L. A. Schaller, L. Schellenberg, E. B. Shera, and C. W. de Jager, At. Data Nucl. Data Tables **60**, 177 (1995).
[8] F. J. Hartmann, R. Bergmann, H. Daniel, H.-J. Pfeiffer, T. von Egidy, and W. Wilhelm, Z. Phys. A **305**, 189 (1982).
[9] P. Vogel, Phys. Rev. A **22**, 1600 (1980).
[10] A. Suzuki, Phys. Rev. Lett. **19**, 1005 (1967).
[11] B. MacDonald, J. A. Diaz, S. N. Kaplan, and R. V. Pyle, Phys. Rev. **139**, B1253 (1965).
[12] F. P. Brady, N. S. P. King, M. W. McNaughton, and G. R. Satchler, Phys. Rev. Lett. **36**, 15 (1976).
[13] H. M. Xu *et al*., Bull. Am. Phys. Soc. **40**, 977 (1995).
[14] National Nuclear Data Center at www.nndc.bnl.gov/ensdf.

[15] P. J. P. Ryan, M. N. Thompson, K. Shoda, and T. Tanaka, Nucl. Phys. **A371**, 318 (1981).
[16] R. K. Sheline and R. A. Harlan, Nucl. Phys. **29**, 177 (1962).
[17] M. Zaider, D. Ashery, S. Cochavi, S. Gilad, M. A. Moinester, Y. Shamai, and A. I. Yavin, Phys. Rev. C **16**, 2313 (1977).
[18] G. H. Miller, M. Eckhause, P. Martin, and R. E. Welsh, Phys. Rev. C **6**, 487 (1972).
[19] T. P. Gorringe, D. S. Armstrong, S. Arole, M. Boleman, E. Gete, V. Kuz'min, B. A. Moftah, R. Sedlar, T. J. Stocki, and T. T. Tetereva, Phys. Rev. C **60**, 055501 (1999).
[20] S. E. Sobottka and E. L. Wills, Phys. Rev. Lett. **20**, 596 (1968).
[21] T. Niizeki *et al*., Nucl. Phys. **A577**, 37c (1994).
[22] D. Frekers *et al*., Groningen Annual Report 2001, p. 1.
[23] J. P. Perroud, Seminar on Electromagnetic Interactions of Nuclei at Low and Medium Energies, Moscow, June 1981; also the SIN Annual Report, 1976, E45. For a more accessible spectrum, see Ref. 4.
[24] B. D. Anderson, N. Tamimi, A. R. Baldwin, M. Elaasar, R. Madey, D. M. Manley, M. Mostajabodda'vati, J. W. Watson, W. M. Zhang, and C. C. Foster, Phys. Rev. C **43**, 50 (1991).
[25] V. A. Kuz'min and T. V. Tetereva, Yad. Fiz. **63**, 1966 (2000); Phys. At. Nucl. **63**, 1874 (2000).
[26] P. M. Endt and C. van der Leun, Nucl. Phys. **A310**, 1 (1978).
[27] R. L. Gulbranson, L. S. Cardman, A. Doron, A. Erell, K. R. Lindgren, and A. I. Yavin, Phys. Rev. C **27**, 470 (1983).
[28] J. E. M. Thomson and M. N. Thompson, Nucl. Phys. **A285**, 84 (1977).
[29] N. Takahashi, Y. Hashimoto, Y. Iwasaki, K. Sakurai, F. Soga, K. Sagara, Y. Yano, and M. Sekiguchi, Phys. Rev. C **23**, 1305 (1981).
[30] B. A. Moftah, Ph.D. thesis, University of British Columbia, 1995 (unpublished).
[31] B. A. Moftah, E. Gete, D. F. Measday, D. S. Armstrong, J. Bauer, T. P. Gorringe, B. L. Johnson, B. Siebels, and S. Stanislaus, Phys. Lett. **B395**, 157 (1997).
[32] R. G. Helmer and C. van der Leun, Nucl. Instrum. Methods A **450**, 35 (2000).
[33] M. S. Dewey, E. G. Kessler, Jr., R. D. Deslattes, H. G. Börner, M. Jentschel, C. Doll, and P. Mutti, Phys. Rev. C **73**, 044303 (2006).
[34] S. Raman (private communication).
[35] Z. Revay (private communication); see also "Database of Prompt Gamma Rays from Slow Neutron Capture for Elemental Analysis", IAEA-STI/PUB/1263, publ. 2007.
[36] K. Shizuma, H. Inoue, and Y. Yoshizawa, Nucl. Instrum. Methods **137**, 599 (1976).
[37] Y. Lee, N. Hashimoto, H. Inoue, and Y. Yoshikawa, Appl. Radiat. Isotopes **43**, 1247 (1992).
[38] G. Fehrenbacher, R. Meckbach, and H. G. Paretzke, Nucl. Instrum. Methods A **372**, 239 (1996).
[39] E. Gete, D. F. Measday, B. A. Moftah, M. A. Saliba, and T. J. Stocki, Nucl. Instrum. Methods A **388**, 212 (1997).
[40] R. Bergmann, H. Daniel, T. von Egidy, F. J. Hartmann, J. J. Reidy, and W. Wilhelm, Z. Phys. A **291**, 129 (1979).
[41] T. Suzuki, D. F. Measday, and J. P. Roalsvig, Phys. Rev. C **35**, 2212 (1987).
[42] J. Vernotte, G. Berrier-Ronsin, S. Fortier, E. Hourani, J. Kalifa, J. M. Maison, L. H. Rosier, G. Rotbard, and B. H. Wildenthal, Phys. Rev. C **48**, 205 (1993).
[43] J. E. M. Thomson, Ph.D. thesis, Melbourne University, 1976, unpublished, data given in Ryan *et al*. [15].
[44] A. Sada *et al*., Nucl. Phys. **A551**, 125 (1993).
[45] D. G. Ireland *et al*., Nucl. Phys. **A554**, 173 (1993).
[46] A. Wyttenbach, P. Baertschi, S. Bajo, J. Hadermann, K. Junker, S. Katcoff, E. A. Hermes, and H. S. Pruys, Nucl. Phys. **A294**, 278 (1978).
[47] L. F. Mausner, R. A. Naumann, J. A. Monard, and S. N. Kaplan, Phys. Rev. A **15**, 479 (1977).
[48] George H. Miller, Ph.D. thesis, College of William and Mary, WM-39-72, 1972 (unpublished).
[49] B. Lawergren and J. Beyea, Phys. Rev. C **6**, 2082 (1972).
[50] H. H. Schmidt, P. Hungerford, H. Daniel, T. von Egidy, S. A. Kerr, R. Brissot, G. Barreau, H. G. Börner, C. Hofmeyr, and K. P. Lieb, Phys. Rev. C **25**, 2888 (1982).
[51] T. A. E. C. Pratt, Nuovo Cimento B **61**, 119 (1969).
[52] J. Vernotte *et al*., Phys. Rev. C **49**, 1559 (1994).
[53] P. M. Endt, Nucl. Phys. **A521**, 1 (1990).
[54] P. M. Endt, Nucl. Phys. **A633**, 1 (1998).
[55] G. G. Bunatyan, V. S. Evseev, L. N. Nitityuk, V. N. Porkrvskii, V. N. Rybakov, and I. A. Yutlandov, Yad. Fiz. **11**, 795 (1970); Sov. J. Nucl. Phys. **11**, 444 (1970).
[56] C. Lüttge, P. von Neumann-Cosel, F. Neumeyer, C. Rangacharyulu, A. Richter, G. Schrieder, E. Spamer, D. I. Sober, S. K. Matthews, and B. A. Brown, Phys. Rev. C **53**, 127 (1996).
[57] C. P. Browne, Phys. Rev. **114**, 807 (1959).
[58] J. Spuller, M. D. Hasinoff, S. T. Lim, D. F. Measday, and T. J. Mulligan, Nucl. Phys. **A248**, 276 (1975).
[59] H. W. Baer, K. M. Crowe, and P. Truöl, Adv. Nucl. Phys. **9**, 177 (1977).
[60] M. Gmitro, R. A. Eramzhian, H. Kissener, and P. Truöl, Sov. J. Part. Nucl. **13**, 513 (1982); **14**, 323 (1983).
[61] M. Lifshitz and P. Singer, Phys. Rev. C **22**, 2135 (1980).
[62] S. S. Dietrich and B. L. Berman, At. Data Nucl. Data Tables **38**, 199 (1988).
[63] E. Kolbe, K. Langanke, and P. Vogel, Phys. Rev. C **50**, 2576 (1994).
[64] J. Hadermann and K. Junker, Nucl. Phys. **A271**, 401 (1976).